AD-A057 663   FLIGHT DYNAMICS RESEARCH CORP VAN NUYS CALIF   F/G 21/5
                END WALL AND CORNER FLOW IMPROVEMENTS OF THE RECTANGULAR ALPERI--ETC(U)
                MAY 78   M ALPERIN, J WU   N62269-77-C-0232
UNCLASSIFIED   NADC-77050-30   NL
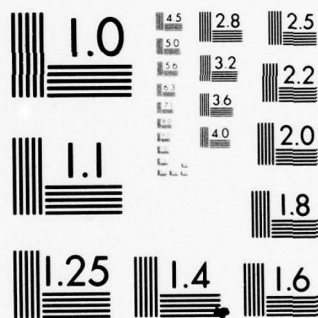
| OF |
AD
A057663

END
DATE
FILMED
9-78
DDC

MICROCOPY RESOLUTION TEST CHART

NATIONAL BUREAU OF STANDARDS-1963-A

LEVEL Ⅱ

NADC-77050-30

END WALL AND CORNER FLOW IMPROVEMENTS
OF THE RECTANGULAR ALPERIN JET-DIFFUSER EJECTOR

by

MORTON ALPERIN and JIUNN-JENQ WU

MAY 1978

PREPARED FOR

D D C
RECEIVED
AUG 15 1978
RECEIVED
D

78 08 11 053

REPORT DOCUMENTATION PAGE		READ INSTRUCTIONS BEFORE COMPLETING FORM
1. REPORT NUMBER NADC - 77050 - 30	2. GOVT ACCESSION NO.	3. RECIPIENT'S CATALOG NUMBER
4. TITLE (and Subtitle) End Wall and Corner Flow Improvements of the Rectangular Alperin Jet-Diffuser Ejector.		5. TYPE OF REPORT & PERIOD COVERED Final Report. May 77 - May 78.
		6. PERFORMING ORG. REPORT NUMBER
7. AUTHOR(s) Morton Alperin Jiunn-Jenq Wu		8. CONTRACT OR GRANT NUMBER(s) N62269-77-C-0232
9. PERFORMING ORGANIZATION NAME AND ADDRESS Flight Dynamics Research Corporation 15809 Stagg Street Van Nuys, CA 91406		10. PROGRAM ELEMENT, PROJECT, TASK AREA & WORK UNIT NUMBERS PE. No. 62241N, F41400 WF41400000, ZA601
11. CONTROLLING OFFICE NAME AND ADDRESS Naval Air Development Center Code 3014 Warminster, PA 18974		12. REPORT DATE May 1978
		13. NUMBER OF PAGES 73
14. MONITORING AGENCY NAME & ADDRESS(If different from Controlling Office) SAME AS BLOCK 11 72p.		15. SECURITY CLASS. (of this report) Unclassified
		15a. DECLASSIFICATION/DOWNGRADING SCHEDULE

16. DISTRIBUTION STATEMENT (of this Report)

Approved for Public Release; Distribution Unlimited

17. DISTRIBUTION STATEMENT (of the abstract entered in Block 20, if different from Report)

SAME AS BLOCK 16

18. SUPPLEMENTARY NOTES

19. KEY WORDS (Continue on reverse side if necessary and identify by block number)
Ejector
Thrust Augmentation
Propulsion
Potential Flow

20. ABSTRACT (Continue on reverse side if necessary and identify by block number)
A generalized ring vortex system was utilized to determine the pressure distributions and streamline shapes within a three-dimensional jet-diffuser ejector.
    Experiments verified the utility of the method and resulted in a measured performance exceeding that of the original STAMP (Small Tactical Aerial Mobility Platform) Ejector, while avoiding the use of the large, protruding end plates required by that ejector.
    Ground effect tests on the new design showed improved performance compared to similar tests on the STAMP Ejector over the entire range of ground clearances.

DD FORM 1473 1 JAN 73   EDITION OF 1 NOV 65 IS OBSOLETE

LEVEL Ⅱ

NADC-77050-30

END WALL AND CORNER FLOW IMPROVEMENTS
OF THE RECTANGULAR ALPERIN JET-DIFFUSER EJECTOR

by

MORTON ALPERIN and JIUNN-JENQ WU

FLIGHT DYNAMICS RESEARCH CORPORATION
15809 STAGG STREET
VAN NUYS, CALIFORNIA 91406

MAY 1978

PREPARED FOR

DDC

RECEIVED
AUG 15 1978
RECEIVED
D

78 08 11 053

PREFACE

The effort reported in this document was performed by Flight Dynamics Research Corporation during the period May 1977 through May 1978. The sponsorship was provided by the Naval Air Development Center, Warminster, Pennsylvania, under Contract No. N62269-77-C-0232. Technical Coordination was provided by Dr. Kenneth Green and Mr. Carmen Mazza of the Naval Air Development Center.

SUMMARY

The objective of this program was to improve the performance characteristics of the "Alperin Jet-Diffuser Ejector" by minimizing the adverse effects caused by the end walls. Analytical predictions have been made to optimize end wall shapes and configurations. These designs were fabricated and applied to the existing jet-diffuser ejector for testing.

The investigation reported in this document was based upon the assumption that the complex flow pattern within an ejector could be treated with sufficient accuracy to provide pressure and pressure gradient data by a potential flow analysis. Pressure distributions at a cross-section midway between the ends of the rectangular STAMP AJDE (Small Tactical Aerial Mobility Platform, Alperin Jet-Diffuser Ejector), with flat semi-circular end plates (to provide essentially two-dimensional flow) were measured in the transverse (x) direction and along the surfaces of the ejector in the flow direction. These pressure distributions were shown to be very similar to those predicted by a two-dimensional, potential flow resulting from the presence of a pair of vortices extending to infinity perpendicular to the flow direction. Differences between the measured and the analytical pressures, although small, could be qualitatively ascribed to the presence of the high stagnation pressure region of the flow from the primary jets, and to the influence of the presence of finite ends in the rectangular ejector. The agreement between theory and experiment is shown to be sufficiently close to justify the use of the method of potential flow.

To investigate the flow properties near the ends of an ejector, where the three-dimensionality is predominant, a closed, rectangular distribution of vortices of constant strength was utilized. Its location and size were chosen such that the resulting streamline at the middle plane closely matched the STAMP ejector's geometric requirement. Velocities, pressures and pressure gradients were determined for a series of such vortex distributions. Of all the choices resulting from this procedure, the one which had a maximum pressure gradient approximately equal to the theoretical maximum pressure gradient of the two-dimensional analysis of the existing STAMP ejector was chosen for fabrication and testing.

The performance of the diffuser configuration (labelled A) based on this vortex arrangement, was almost equivalent to that of the STAMP AJDE ejector with semi-circular end plates. Thus the need for the protruding, high drag end plates was eliminated with very little penalty in performance.

Observation of the flow in the diffuser of Configuration A indicated the presence of a large distortion of diffuser jet thickness around the exit of the diffuser, which was attributed to the large difference in maximum pressure gradients (and therefore of absolute or gage pressure) among the various stream-lines originating at the different peripheral locations around the diffuser, and different amounts of surface divergence among different diffuser jet stream tubes. Therefore, despite the absence of observable separation, the peripheral variation of maximum pressure gradients resulted in a cross flow and a performance penalty. To minimize these peripheral pressure gradients, the rectangular distribution of vortices was replaced by a more flexible pattern providing a three-dimensional relocation of corners.

A lengthy computer analysis, aimed at the determination of the vortex arrangement which minimized the difference in the maximum pressure gradients among the different streamlines, was carried out. Other conditions, known from previous experience to be essential for effective jet-diffusion, were also imposed upon the selection of the most suitable vortex distribution. The results are described in detail along with the selection criteria and properties of the selected arrangement.

After fabrication, the ejector with this diffuser (Configuration B) was tested and the results presented as a function of primary nozzle position and orientation.

At $A_2/(s_\infty + a_\infty) = 21$, the ejector was relatively small and had a large ratio of diffuser jet slot thickness to primary jet slot thickness, but the experiment produced a maximum thrust augmentation of 2.13. This exceeds the performance of the STAMP AJDE at equivalent geometric conditions, despite the elimination of the end plate.

Smaller values of s_∞/a_∞ would be desirable but would require a redesign of the diffuser to avoid excessive skin friction in the solid portion of the diffuser. In other words, this requires a shorter diffuser.

Results of comparative tests of the Configuration B ejector with an equiv-
alent STAMP AJDE in ground proximity are also presented. The improved performance
of Configuration B, compared to the STAMP AJDE, over the entire range of distances
between ejector and ground plane is clearly shown to result from the minimization
of the adverse effects caused by the flat end walls of the STAMP Ejector.

LIST OF SYMBOLS

A_2	Cross section area of ejector at throat
a_∞	Primary nozzle exit area when mass flow is expanded to ambient pressure
a,b,c da,db,dc	Dimensions of vortex distribution (see Figure 8)
E,F,G,H $\underline{E},\underline{F},\underline{G},\underline{H}$ $\overline{EF},\overline{GH}$	Corners of vortex distribution (see Figure 8)
L	Length of throat of ejector
$\dot{m}$	Mass flow
p	Pressure (gage)
P_o	Stagnation pressure (gage) for both primary and diffuser jet
P_{CL}	Pressure (gage) at ejector's center
P_∞	Ambient Pressure
s	Curvilinear distance along streamlines
s_∞	Diffuser jet exit area when expanded from P_o to ambient pressure (p_∞)
t_p	Thickness of primary jet slot
t_d	Thickness of diffuser jet slot
$\vec{V}$	Velocity vector
u,v,w	Components of velocity vector
x,y,z	Coordinates
X_2	Throat width of ejector
z_o	Distance from ejector's throat to diffuser jet (in thrust direction)
z_e	Distance from ejector's throat to end of solid surface (in thrust direction)
β_o	Angle of diffuser surface to thrust direction, at diffuser jet
β_e	Angle of diffuser surface to thrust direction, at end of solid surface
δ	Diffuser area ratio
ϕ	Thrust augmentation = ejector net thrust/isentropic reference jet net thrust. Reference jet has jet power and mass flow equal to those of injected gases of ejector
ξ,η,θ	Position and orientation of primary nozzles (see Figures 1 and 4)
Γ	Circulation

LIST OF FIGURES

TABLE OF CONTENTS

I INTRODUCTION

Ejectors to be utilized for stationary or low speed thrust, as for V/STOL applications, require large diffuser area ratios to achieve high thrust augmentation. The achievement of large effective diffuser area ratios in an adverse pressure gradient requires solid surfaces which diverge at a small angle if flow separation is to be avoided, or alternatively, some type of boundary layer control is necessary if surfaces diverge rapidly.

The jet-diffuser ejector is one concept developed specifically for ejectors, which has demonstrated a capability for avoiding separation in solid diffuser surfaces with divergence half-angles in excess of 45 degrees. In addition, the diffuser jet, if properly designed, provides a means for extending the diffusion process for a considerable distance downstream of the solid surfaces. Further, the process of mixing of primary injected fluid with the flow induced from the environment, essential for thrust augmentation, can be provided with additional length for its effective culmination in the jet-diffuser without the requirement for long solid surfaces. This is in direct contrast to the essential termination of the effective mixing process at the end of the solid surfaces of a conventional diffuser.

Although in a two-dimensional sense the concept of jet diffusion and its intrinsic advantages are clear, the essential practical requirements of three-dimensionality or finite aspect ratio of ejectors, introduces some complex aerodynamic problems. These three-dimensional aspects of jet diffusion, or end effects, are the subject of the investigation reported in this document.

II JET-DIFFUSION CONCEPT

The concept of jet-diffusion is basically an extension of the concepts of boundary layer control by the use of blowing jets and of the jet flap to provide additional diffusion beyond that of the solid surfaces. Blowing jets have been used to delay separation in large area ratio solid diffusers with some degree of success. By blowing a jet having a higher stagnation pressure than the ambient pressure in the diffuser, separation can be delayed to the point where the effective diffuser area ratio is almost as large as the geometric area ratio of the solid surface. Using energized fluid for the avoidance of separation is a costly process, since the momentum of the boundary layer control fluid must be considered in the evaluation of ejector performance. Thus, unless extreme care is exercised in the design of the blowing jet system, the net effect can be more detrimental than that of the use of a smaller diffuser area ratio without boundary layer control.

Jet diffusion has the advantage over conventional blowing jet systems in that it has the potential for providing a diffuser area ratio larger than the geometric area ratio of the solid surfaces in addition to its capability for avoiding separation despite extremely large divergence angles of the solid surfaces. A typical jet diffuser ejector developed under the U.S. Navy/Marine Corps STAMP (Small Tactical Aerial Mobility Platform) Program and tested at the Naval Air Propulsion Center is illustrated on Figure 1. This ejector was the result of an intensive development program aimed at its eventual use as the lifting, thrusting and controlling element of an apterous vehicle and details of its development program and its performance are described in Reference 1. It is of particular interest to note that, as shown on Figure 1, the ends of the ejector are flat, with a semi-circular end plate protruding beyond the solid diffuser surfaces at the ends of the ejector as a means of providing two-dimensional flow in the diffuser.

ALPERIN JET-DIFFUSER EJECTOR
Model 0542
1976

Figure 1

FLIGHT DYNAMICS RESEARCH CORP. Van Nuys, Cal.
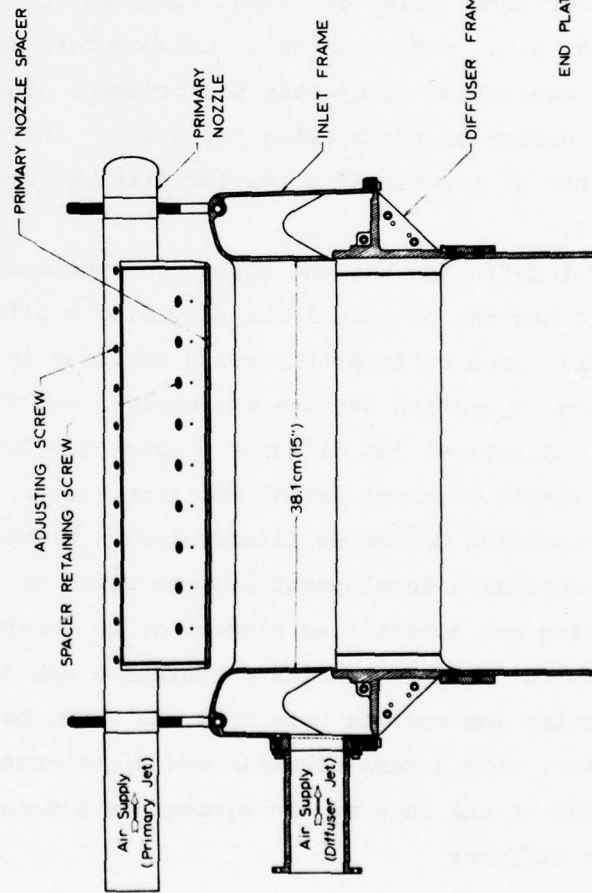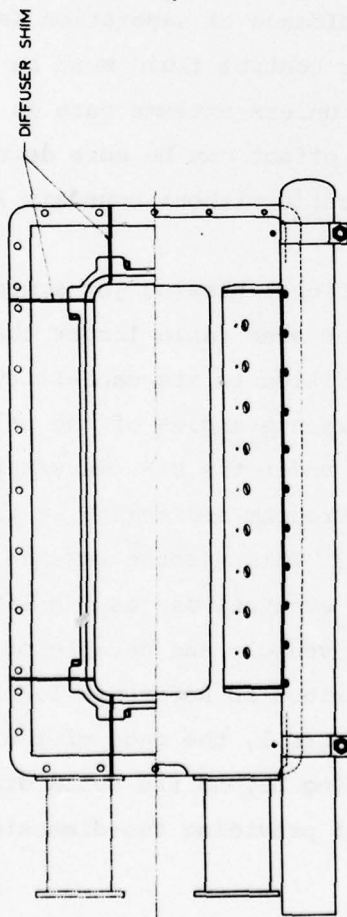
This protruding end plate, although somewhat undesirable from the view-
point of ejector integration and drag characteristics,was essential for the
avoidance of some performance degradation associated with the use of flat ends
within the diffuser.

Attempts to utilize diverging end bells resulted in local flow separation
and performance penalties not acceptable under the STAMP Program and the design
illustrated on Figure 1 was utilized as a quick-fix alternative. The advantage
resulting from the use of end plates is best illustrated by perusal of the data
presented on Figures 2 and 3. To illustrate the characteristics of the flow
within the region of jet diffusion, the pressure distribution in that region is
plotted on Figure 2 with a large end plate extending from the end of the solid
diffuser to a distance of 27.4 cm, or 0.9 of the exit dimension. Obviously, the
recovery of kinetic energy attributable to the jet diffuser is directly related to
the pressure recovery in the region illustrated by the isobars. Removal or re-
duction in size of the end plate would seriously collapse the isobar pattern
and cause a pressure increase throughout the ejector, with an accompanying re-
duction in secondary/primary flow ratio and thrust augmentation.

The influence of end plate size on the thrust augmentation of the ejector,
with a geometric diffuser area ratio of 3, is plotted on Figure 3. The semi-
circular end plate (labelled STAMP) is shown to produce a thrust augmentation
factor of 2.12 with the illustrated ejector and end plate configuration. In-
creasing the end plate to a 27.4 cm x 61 cm shape similar to that used in Fig-
ure 2 resulted in an increase of 3% or a thrust augmentation of 2.18. Decreasing
the end plate size resulted in a more serious performance degradation, equivalent
to a reduction of 14% in the thrust augmentation, to a value of 1.82.
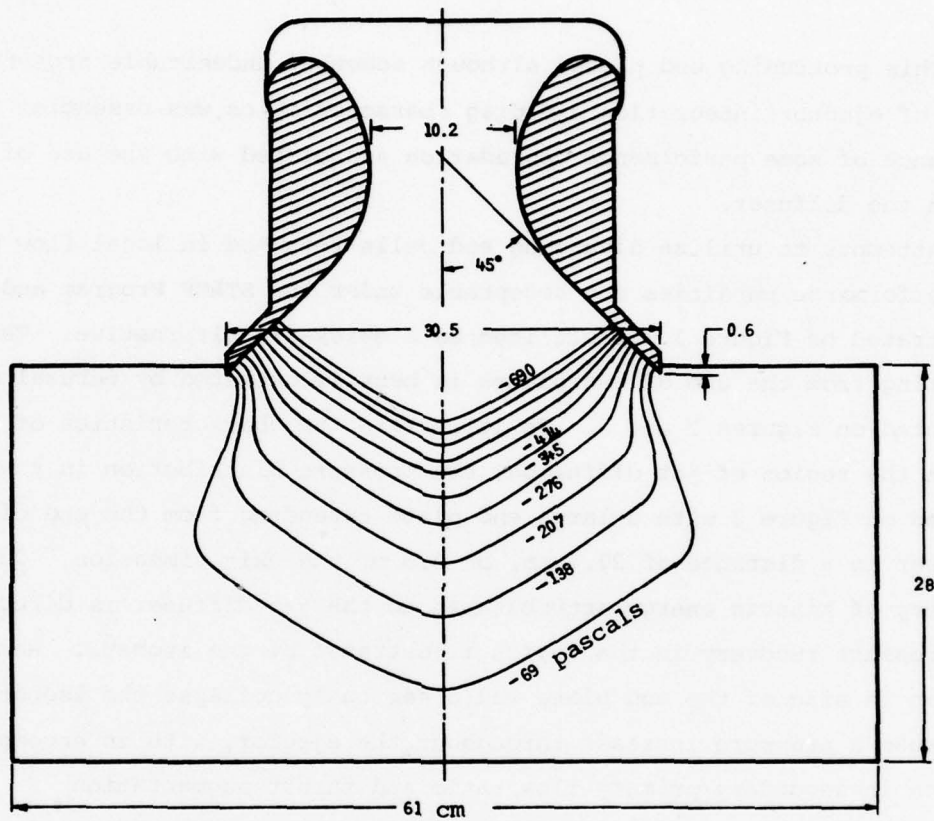
Figure 2. ISOBARS ON END PLATE OF STAMP AJDE EJECTOR

$P_o = 24.3$ kilopascals; $A_2/(s_\infty + a_\infty) = 21.6$; $s_\infty/a_\infty = 0.62$
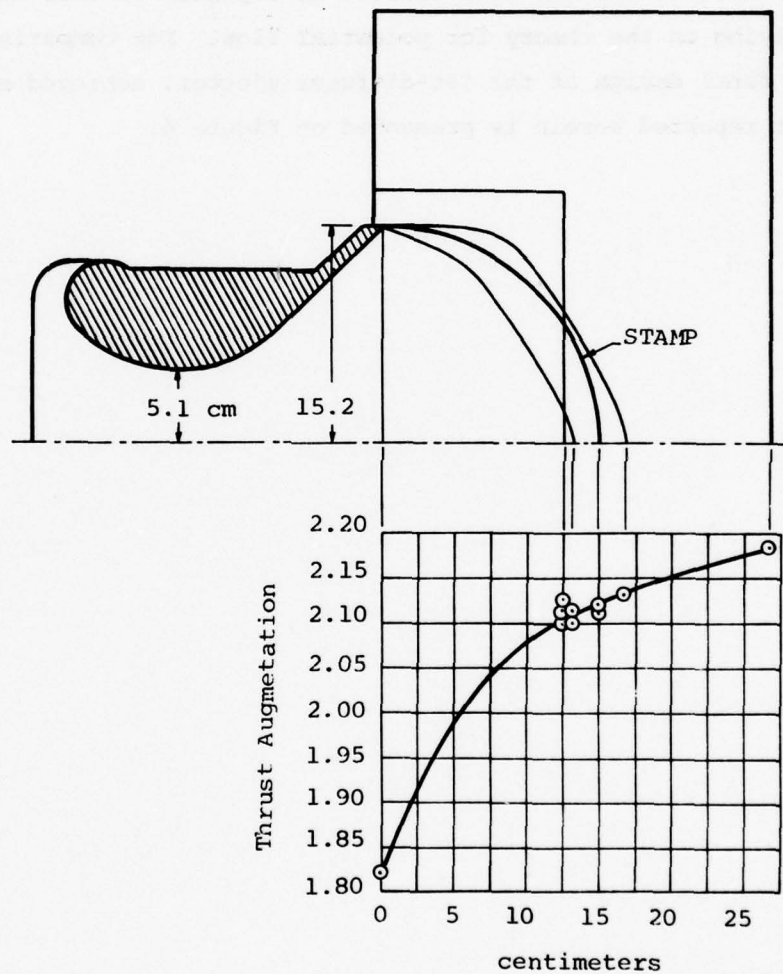
Figure 3.   END PLATE CONFIGURATION AND PERFORMANCE

P_o = 24.3 kilopascals; $A_2/(s_\infty + a_\infty)$ = 21.6; s_∞/a_∞ = 0.62

The use of a flat end in conjunction with a protruding end plate was a quick-fix for a complex problem whose solution could not be undertaken during the STAMP Program due to scheduling limitations. It was therefore relegated to further efforts and has been treated as reported in this document by a method relying on the theory for potential flow. For comparison and reference, the final design of the jet-diffuser ejector, achieved as a result of the effort reported herein is presented on Figure 4.

ALPERIN JET-DIFFUSER EJECTOR

Model 0232

1978

FLIGHT DYNAMICS RESEARCH CORP. Van Nuys, Cal.
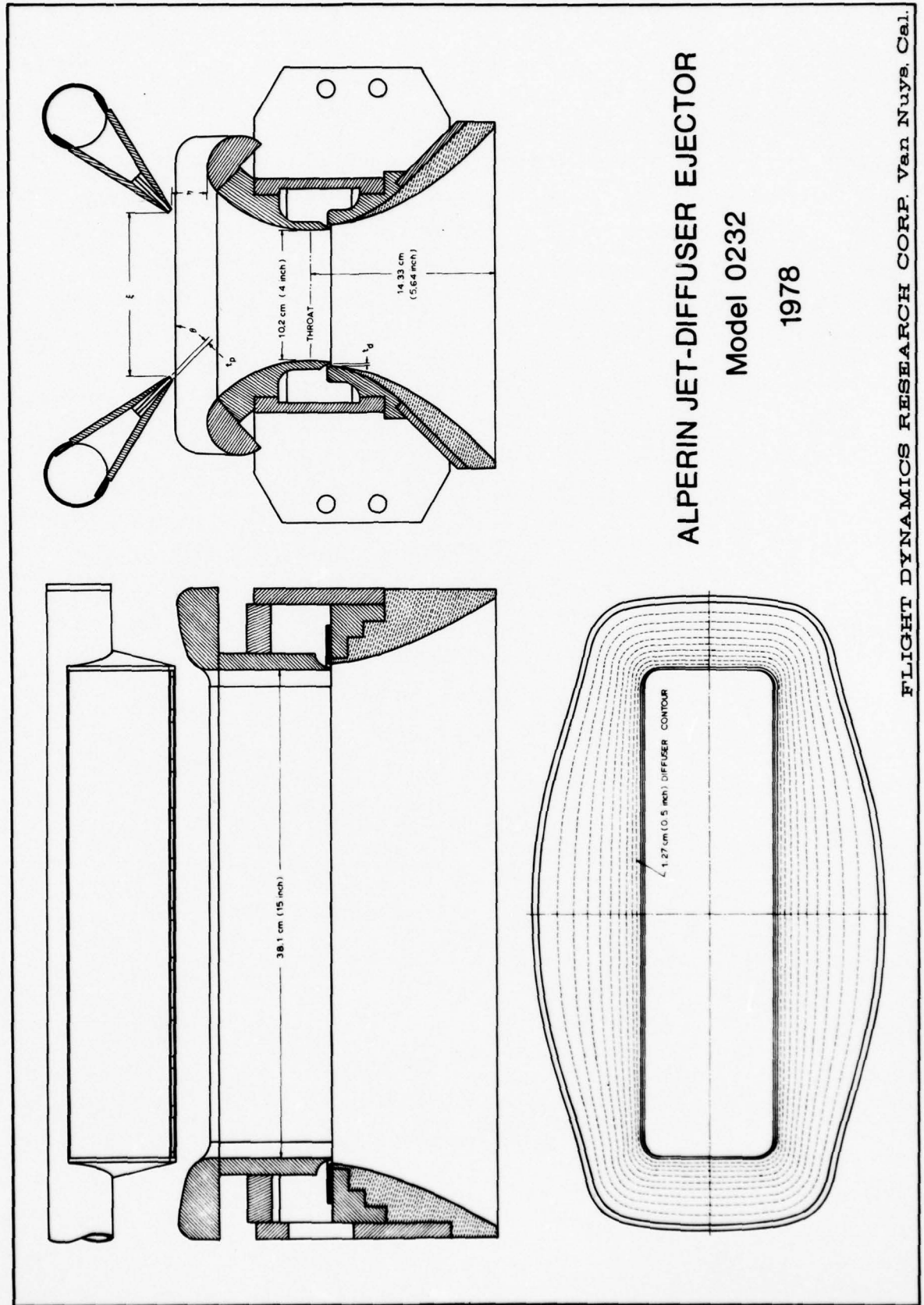
Figure 4

III POTENTIAL FLOW ANALYSIS

1. Two-Dimensional Considerations

The flow field within a two-dimensional ejector may be approximated by the application of the vortex theory commonly used to describe the flow field around aircraft wings. Under the assumptions of irrotational, inviscid, incompressible flow, the surface of the ejector can be approximated by the streamlines resulting from the presence of pairs of vortex distributions. To illustrate the technique, consider an ejector of the AJDE type.

This ejector consists of two cylindrical surfaces of radius R, on each side, separated by the throat width X_2, as shown on Figure 5
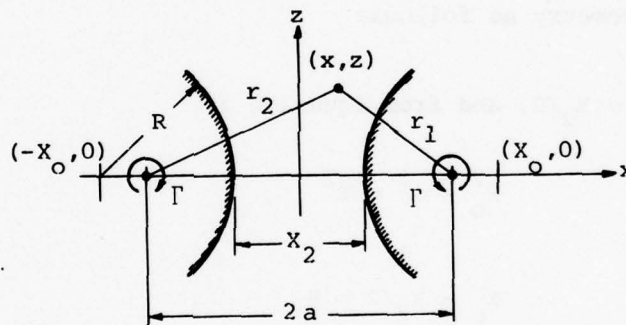
Figure 5.   MID-SECTION OF AN AJDE

and can be represented by two counter rotating vortices of infinite extent in the y direction, separated by the distance "2a", in the x direction and symmetric with respect to the z axis, as illustrated.

The stream function for this arrangement is (Reference 2):

$$\psi = (\Gamma/2\pi)\ln(r_1/r_2) \tag{1}$$

or in cartesian coordinates

$$\psi = (\Gamma/4\pi)\ln \frac{z^2 + (x - a)^2}{z^2 + (x + a)^2} \tag{2}$$

Equation 2 can be rewritten as,

$$(x - X_o)^2 + z^2 = X_o^2 - a^2 \qquad (3)$$

where

$$X_o = a \left[\frac{1 + \exp(4\pi\psi/\Gamma)}{1 - \exp(4\pi\psi/\Gamma)} \right] \qquad (4)$$

Equation 4 indicates that for any given streamline (ψ = constant), X_o is a constant, and the relation 3 is a circle, which is a desired solution.

Since the ejector surface is a streamline, the dimension "a" can be related to the ejector geometry as follows:

At $z = 0$, $x = X_2/2$, and from Equation 3,

$$X_o^2 - a^2 = R^2 \qquad (5)$$

but

$$X_o - X_2/2 = R \qquad (6)$$

therefore,

$$a = (X_2/2) \sqrt{1 + 4R/X_2} \qquad (7)$$

For the special case of the STAMP ejector in which $R = X_2$,

$$a = \sqrt{(5/4)} X_2 \qquad (8)$$

With the known location of the vortex lines, the velocity field can be calculated by means of the Biot-Savart law, (Reference 3) and the pressure distribution can be derived from the velocity field, using Bernoulli's Equation.

To establish the validity of the method for simulation of the ejector flow field by a flow field resulting from a prescribed distribution of vortex elements, the pressure distributions along the STAMP ejector's plane of symmetry, its surface and across its throat were measured at its middle plane. These pressure distributions were then compared with the pressure distributions determined analytically from a two-dimensional analysis of an inviscid irrotational, incompressible flow resulting from a pair of infinite vortex filaments.

The analysis was carried out using the geometry of the STAMP AJDE, namely $X_2 = R = 10.2$ cm, which results in the value $a = 11.4$ cm, (Equation 8). In terms of the coordinate system described on Figure 5, the pressure at any point (x,z) within the two-dimensional space can be found from Bernoulli's Equation

$$p = -(\rho/2)V^2 = -\Gamma^2 f(x,z) \tag{9}$$

where

$$f(x,z) = (\rho/8\pi^2) \left\{ z^2 \left[\frac{1}{z^2+(x-a)^2} - \frac{1}{z^2+(x+a)^2} \right]^2 + \left[\frac{a-x}{z^2+(x-a)^2} + \frac{a+x}{z^2+(x+a)^2} \right]^2 \right\} \tag{10}$$

Under the above conditions, the pressure (p) at the ejector's throat $(z = 0)$ is described by the relationship

$$p = -\Gamma^2 \rho/(2\pi^2) \left[\frac{a}{x^2 - a^2} \right]^2 \tag{11}$$

A least square curve fitting technique to evaluate the circulation Γ of a typical STAMP ejector arrangement, provided the value $\Gamma = 32.3$ m^2/sec. With this value for Γ, the theoretical and experimental pressure distributions across the ejector's throat, at its middle plane, are compared on Figure 6.
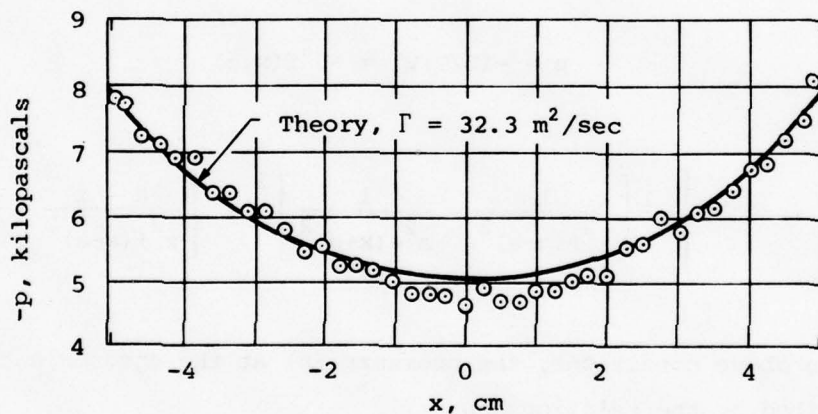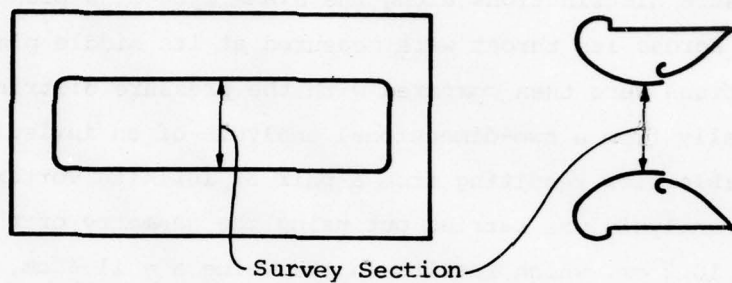
Test Conditions:

$P_o = 24.4$ kilopascals; $\delta = 2.2$; $\beta_e = 45°$;

$A_2/(s_\infty + a_\infty) = 18$; $s_\infty/a_\infty = 0.55$

Figure 6. SURVEY ACROSS AJDE THROAT - AT MIDDLE PLANE
COMPARED TO 2-D THEORY

As illustrated, the theoretical pressure distribution is in close agreement with the experiment, with a small deviation near the side walls ($x = \pm 5$ cm) and at the center ($x = 0$). The excessive pressure at the center and the reduced pressure near the walls are attributed to the influence of the centrifugal force of the higher energy primary fluid near $x = \pm 2.5$ cm.

At the plane of symmetry ($x = 0$), the theoretical values of the pressure distribution are expressed by the relationship

$$p = -\Gamma^2 \rho / (2\pi^2) \left[\frac{a}{z^2 + a^2} \right]^2 \tag{12}$$

Using a least square fitting technique again, the circulation was determined to have a value Γ equal to 29.1 m^2/sec.

A comparison of the theoretical and experimental pressure distribution at $x = 0$ is illustrated on Figure 7, using both values of the circulation determined as described above. As indicated on Figure 7, the theoretical pressure distribution indicates a slower pressure recovery than that measured experimentally. This discrepancy is attributed to the three-dimensionality of the flow field, which with flat ends causes a more rapid deterioration of the jet diffusion process than would occur in a two-dimensional case, or an ejector with a larger aspect ratio. It is also shown on Figure 7 that the end wall pressure is smaller in the absolute scale than that of the two-dimensional theory, with a sudden increase in the vicinity of the diffuser jet. This is a further indication of the adverse end effect, whereby the required pressure gradient exceeds that of the sides of the ejector.
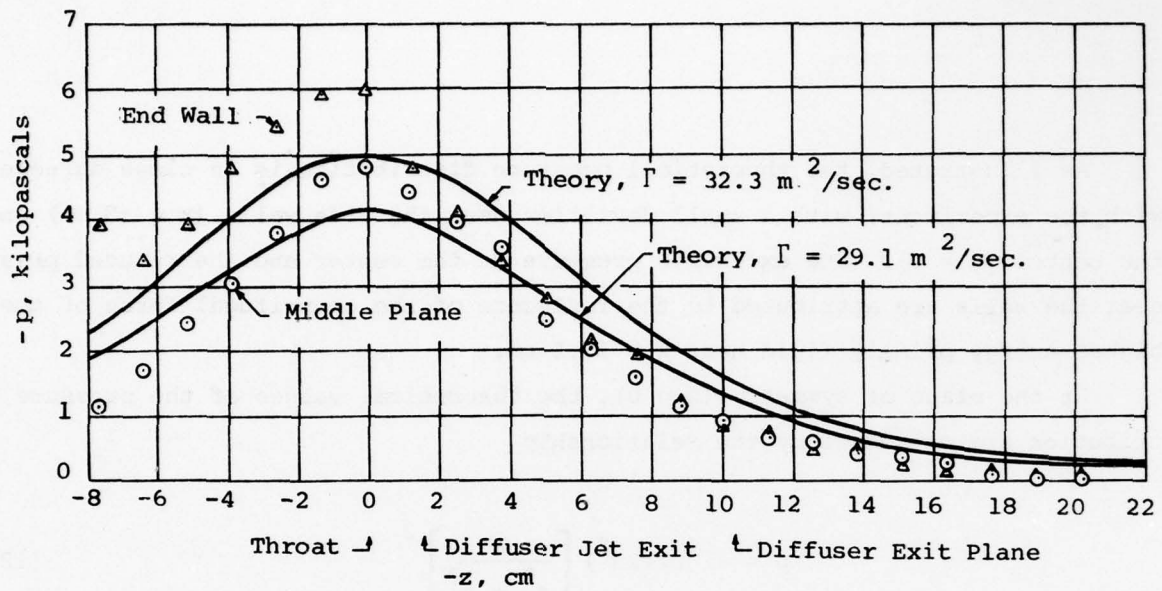
a. PRESSURE DISTRIBUTIONS AT PLANE OF SYMMETRY
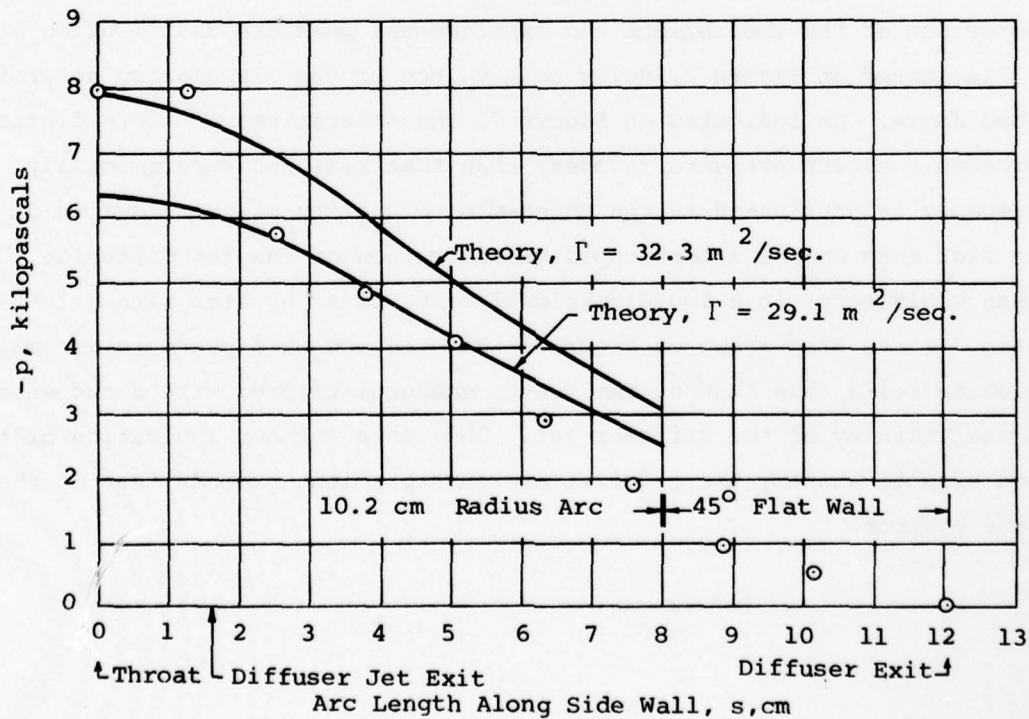
P_O = 24.4 kilopascals; δ = 2.2; s_∞/a_∞ = 0.55; $A_2/(s_\infty + a_\infty)$ = 18; $\beta_e = 45^\circ$

b. PRESSURE DISTRIBUTIONS ON EJECTOR SURFACES AT MIDDLE PLANE

Figure 7.   LONGITUDINAL PRESSURE SURVEYS - STAMP AJDE

Figure 7 also illustrates a comparison of theory and experiment at the ejector middle plane surfaces where

$$x = \pm\{R + (X_2/2) - \sqrt{R^2 - z^2}\} \tag{13}$$

Using this relationship and the two values of Γ determined as described above, the pressure distribution along the ejector surfaces was calculated from Equations 9 and 10. The results are plotted in comparison to the experimental data on Figure 7. At this region the experimental pressure gradient is again shown to be larger than the theoretical, a fact which is again attributed to the finite aspect ratio of the ejector, compared to a two-dimensional analysis.

Based on the survey results, the pressure field is accurately described by potential flow despite the existence of a complex rotational flow field consisting of the primary and induced flows and the mixing process. This may be the result of the large ratio of induced to primary mass flow. With this correlation as a background, the vortex analysis was modified to simulate the three-dimensional reality of the finite aspect ratio ejector.

2. Three-Dimensional Considerations

The deviation of the flow field measurements on the STAMP AJDE Ejector from the two-dimensional potential flow analysis is a consequence of the shedding of trailing vortices near the corners of the rectangular ejector where the uniformity of circulation is interrupted.

According to the Helmholtz theorem, the shedding of trailing vortices and their influence on drag can be avoided by the use of closed vortex distributions of constant circulation. Following this theorem, a generalized ring vortex system of constant circulation, arranged as shown on Figure 8, is adopted. This arrangement is basically a rectangular ring vortex, with the provision to relocate its corner in a three-dimensional fashion.

This generalized ring vortex system consists of six independent parameters: a; b; c; da; db; and dc. But there are two geometric requirements on the middle plane of the ejector:

1. Flow angle (β_o) at the diffuser jet location (x_o, y_o, z_o);

2. Diffuser exit angle (β_e) at a specified diffuser area ratio $(2x_e/X_2)$.

Therefore, only four free parameters can be varied for numerical experiments. The four independent parameters used in this document are b; da; db; and dc, while "a" and "c" are determined by the middle plane requirements. Using this general formulation, the local velocity vector and pressure can be evaluated in the following manner.
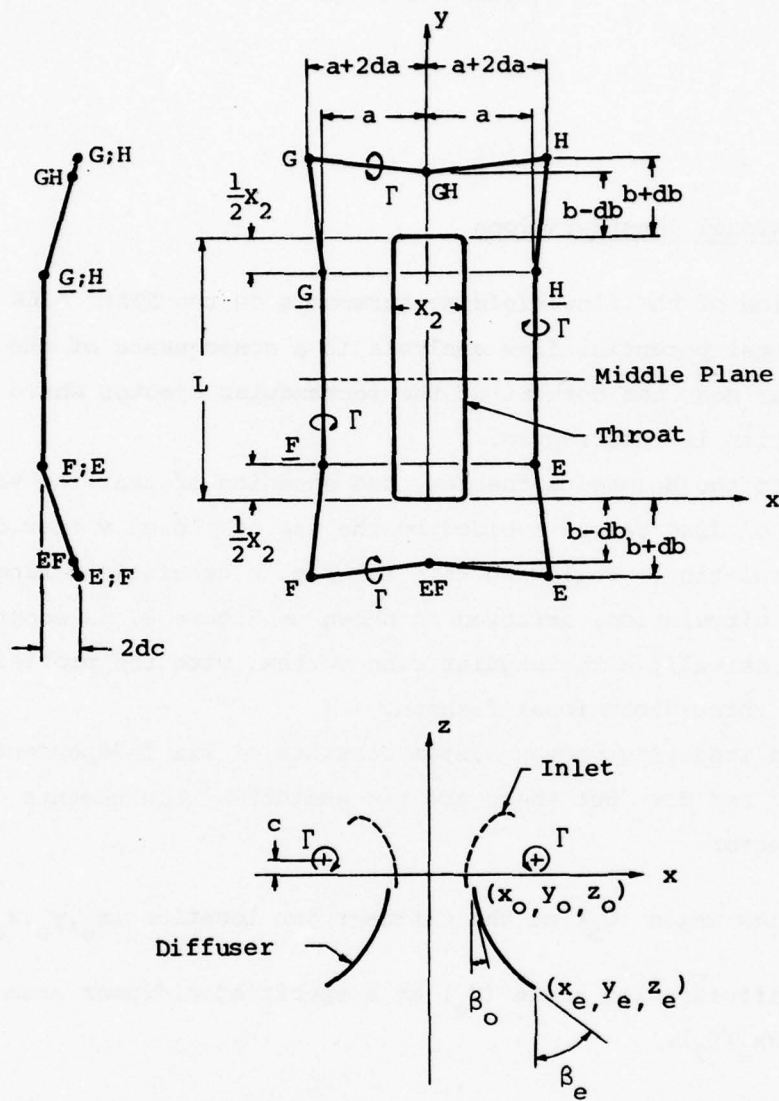
Figure 8. COORDINATE SYSTEM

a. Numerical Method

For any vortex element between points A and B (Figure 9), the velocity at any special point P induced by the vortex element is given by the vector relationship (Reference 3).

$$\vec{v} = (\Gamma/4\pi h)(\cos\theta_1 + \cos\theta_2)\vec{n} \tag{14}$$

where

$\quad\quad\quad\quad \vec{n}$ is the unit vector normal to plane ABPA

$\quad\quad\quad\quad h$ is the distance between point P and the line AB

$\quad\quad\quad\quad \theta_1$ is the angle PAB

$\quad\quad\quad\quad \theta_2$ is the angle PBA
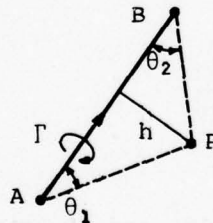
Figure 9. VECTOR DIAGRAM

For the purpose of numerical solution, expressions for $\vec{n}$, h, and the cosine terms are written as follows.

Define the cross product of two unit vectors as,

$$\vec{q} = \frac{\vec{AB}}{|\vec{AB}|} \ \text{x} \ \frac{\vec{AP}}{|\vec{AP}|} = \sin \theta_1 \ \vec{n} = |\vec{q}| \ \vec{n} \tag{15}$$

hence

$$\vec{n} = \frac{\vec{q}}{|\vec{q}|} \tag{16}$$

and

$$h = |\vec{AP}| \ \sin \theta_1 = |\vec{AP}||\vec{q}| \tag{17}$$

and the cosine terms may be expressed as,

$$\cos \theta_1 = \frac{\vec{AB}}{|\vec{AB}|} \cdot \frac{\vec{AP}}{|\vec{AP}|} \tag{18}$$

$$\cos \theta_2 = - \frac{\vec{AB}}{|\vec{AB}|} \cdot \frac{\vec{BP}}{|\vec{BP}|} \tag{19}$$

Substituting Equations 16, 17, 18, and 19 into Equation 14 gives the velocity field induced by the vortex segment as

$$\vec{V} = \{\frac{\Gamma}{4\pi}\}\{\frac{\vec{q}}{|\vec{AP}||\vec{q}|^2}\}\{\frac{\vec{AB}}{|\vec{AB}|} \cdot \frac{\vec{AP}}{|\vec{AP}|} - \frac{\vec{AB}}{|\vec{AB}|} \cdot \frac{\vec{BP}}{|\vec{BP}|}\} \tag{20}$$

With a knowledge of the velocity field, the streamlines (shape of the ejector duct) can be determined as follows.

Since by the definition of a streamline,

$$dx : dy : dz = u : v : w \tag{21}$$

where u, v, and w are the components of the velocity vector in the x, y, and z directions respectively.

Therefore,

$$dx/dz = u/w \tag{22}$$

$$dy/dz = v/w \tag{23}$$

and the streamline is given by,

$$x = x_o + \int_{z_o}^{z} (u/w)\,dz \tag{24}$$

$$y = y_o + \int_{z_o}^{z} (v/w)\,dz \tag{25}$$

For stationary ejectors, the pressure distribution can now be determined with the aid of Bernoulli's Equation, as follows.

$$p = p_{abs} - p_{\infty} = -(\rho/2)\,|\vec{V}|^{2} \tag{26}$$

where

p = gage pressure

p_{abs} = absolute pressure

$$\vec{V} = (u,v,w) \tag{27}$$

or

$$p = -(\rho/2)\,(u^2 + v^2 + w^2) \tag{28}$$

The knowledge of the pressure and velocity distributions for any given choice of vortex distribution, permits the adjustment of the vortex to that which represents a suitable flow pattern. From this choice, the diffuser shape can be established.

b. Configuration A

In the analyses of the flow resulting from a vortex distribution, the boundary conditions were

$$\beta_o = 9.61 \text{ degrees}$$
$$\beta_e = 45 \text{ degrees @ } 2x_e/X_2 = 2.5$$
$$X_2 = 10.16 \text{ cm}$$

at the middle plane of the ejector, to simulate the geometry of the STAMP AJDE Ejector. The vortex strength or circulation (Γ) was maintained constant and fixed for all vortex elements.

Initially, the simplest case of a rectangular ring vortex where da=db=dc=0 was treated by the method described, to determine the streamline shapes and pressure distributions. A set of values of "b" was chosen, where b varied from 6.35 cm to 11.43 cm in intervals of 0.635 cm. For each choice of b, the values of "a" and "c" which satisfied the boundary conditions were determined by an iteration procedure. The details of this procedure are presented in Part I of Appendix B.

For each of the 9 choices of b, the shape and pressure distribution was determined for 20 streamlines, originating at the diffuser jet slot at peripheral locations from the middle plane to the center plane of the end of the ejector by an integration process along each streamline until the prescribed $\beta_e = 45^\circ$ was reached.

For example, the results of the gage pressure distribution (p/p_{CL}) of three selected streamlines originating from the middle plane, the center plane of the end of the ejector, and the corner are presented on the top chart of Figure 10. These pressure distributions were then differentiated numerically to obtain the pressure gradient as shown on the bottom chart of Figure 10. The complete listing of the computer program as well as sample input and output are presented in Part II of Appendix B.
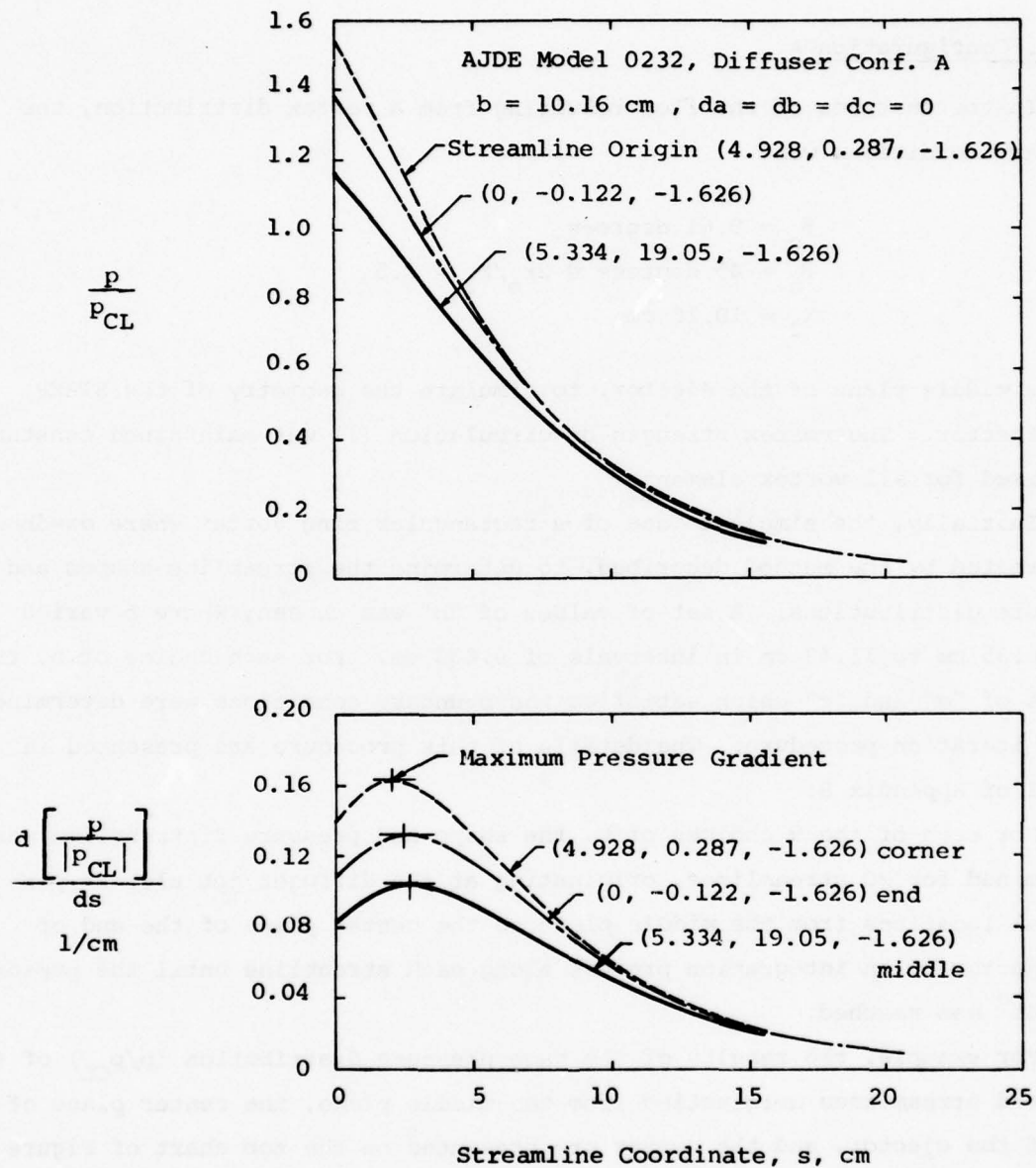
Figure 10. PRESSURE DISTRIBUTIONS AND GRADIENTS
OF SELECTED STREAMLINES OF
CONFIGURATION A

It is important to note that the use of dimensionless pressure (p/p_{CL}), made dimensionless by use of the gage pressure (p_{CL}) at the ejector's center $(0, 19.05, 0)$, provides results which are independent of plenum pressure, since all gage pressures are approximately proportional to the gage plenum pressure.

As a means for evaluating the relative merits of the various Configurations generated by the variation of "b" the maximum pressure gradient for each streamline was plotted vs. streamline origin location on Figure 11. The fact that the maximum pressure gradient is located at the corners of the ejector is clearly evident from perusal of this figure. It is also evident that the magnitude of the maximum pressure gradient decreases with increasing values of b.

The maximum pressure gradient with b = 10.160 cm is closely equivalent to the theoretical maximum pressure gradient of a two-dimensional vortex distribution which produces a streamline corresponding to the design of the STAMP Ejector. Reduction of this maximum pressure gradient by a choice of larger values of b would result in a *longer diffuser*. *Therefore* b = 10.160 cm was chosen for fabrication, and designated as Configuration A.

Contour lines of Configuration A at 1.27 cm spacing are shown on Figure 12.

The measured performance of the ejector with diffuser Configuration A is illustrated on Figure 13 as a function of the position of the primary nozzle and the area ratio $A_2/(s_\infty + a_\infty)$ at a plenum pressure of 24.1 kilopascals (gage).

As illustrated, the thrust augmentation reached a value of 2.01 at optimal values of the primary nozzle position (ξ, η), orientation (θ) and the area ratio $A_2/(s_\infty + a_\infty)$.

The use of a rectangular ring vortex where da = db = dc = 0, resulted in an ejector configuration whose performance, without an end plate, was almost equivalent to that of the STAMP AJDE ejector with semi-circular end plates. However, large peripheral pressure gradients in the diffuser, distort the effective diffuser jet thickness at the exit of the diffuser and limit the proper functioning of the jet-diffuser.
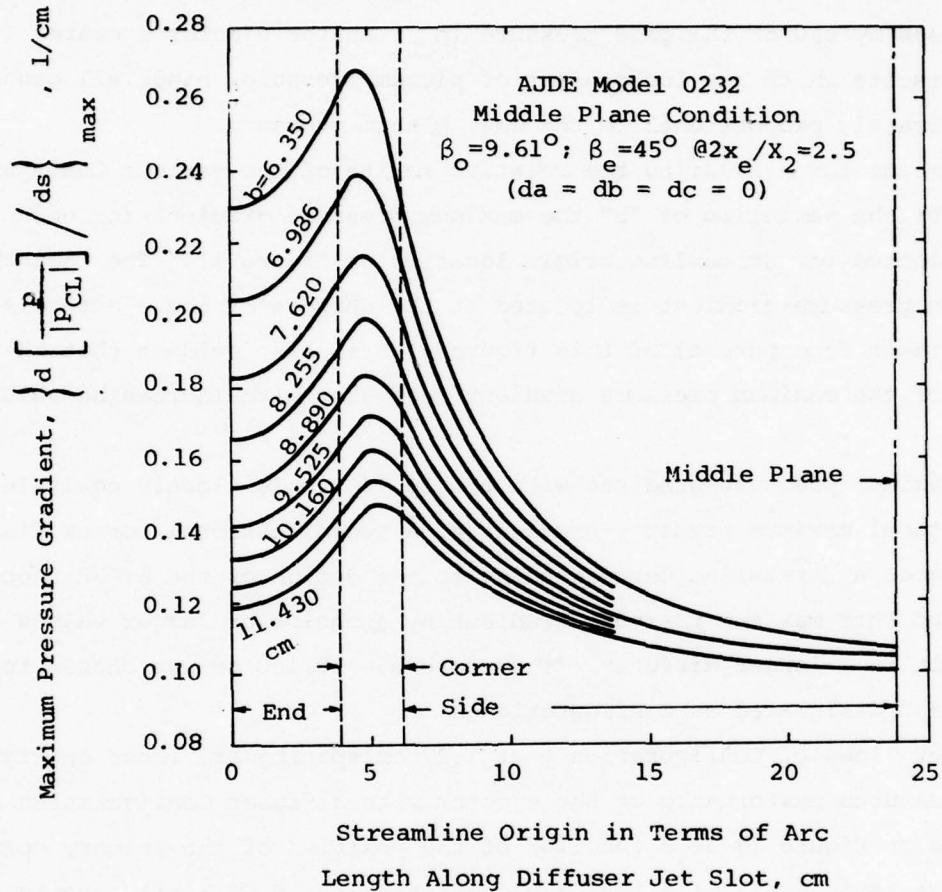
Figure 11. MAXIMUM PRESSURE GRADIENTS FOR DIFFUSER
REPRESENTED BY RECTANGULAR RING VORTICES

CONTOUR LINES (1.27 cm SPACING)
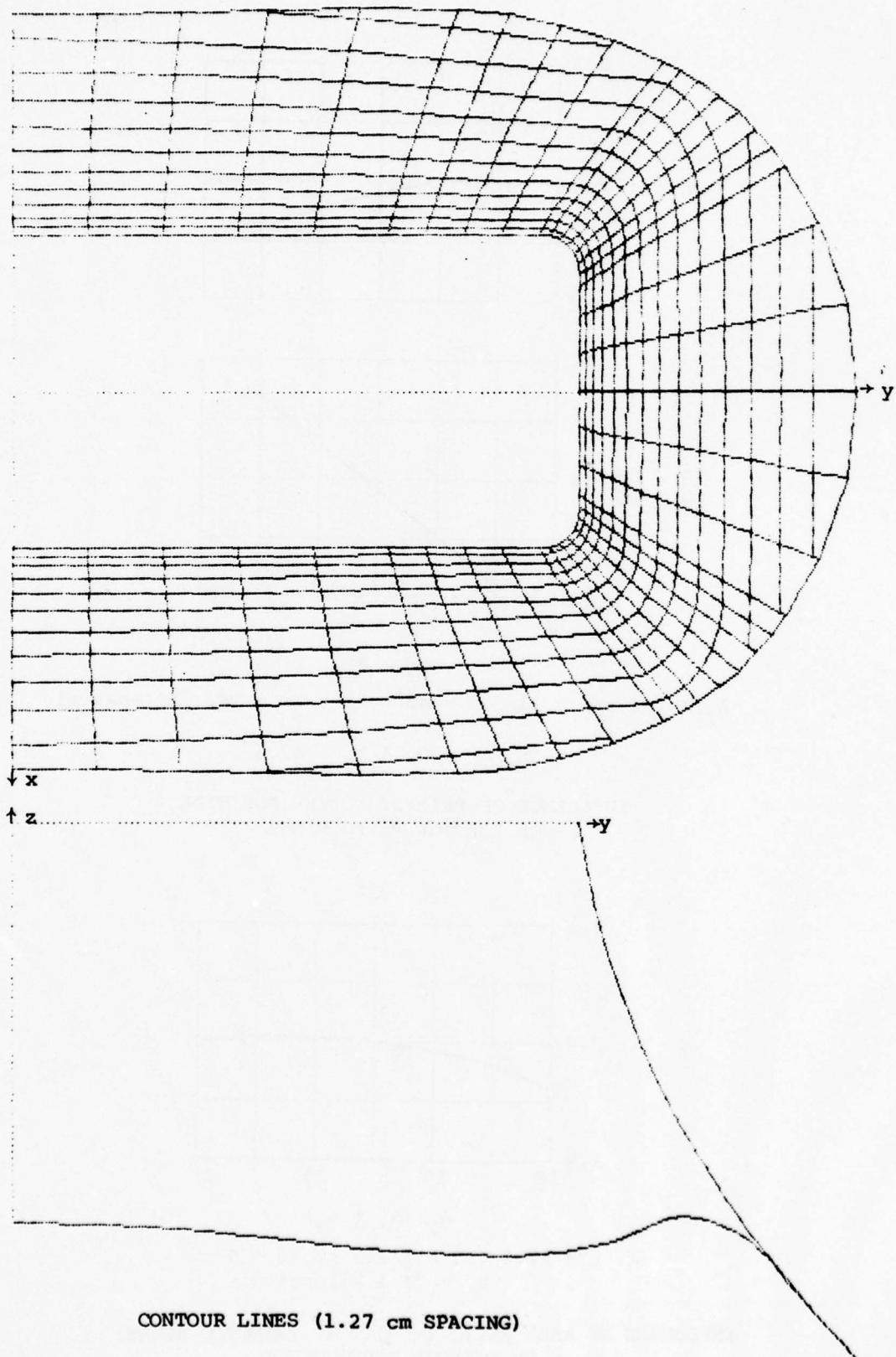
Figure 12. DIFFUSER CONFIGURATION A
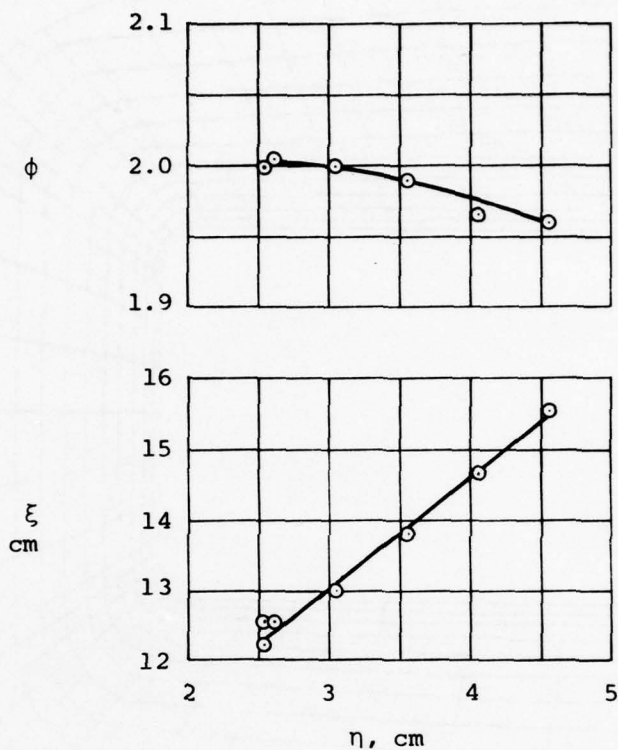
$A_2/(s_\infty + a_\infty) = 21$; $\beta = 45^\circ$; $P_0 = 24.1$ kilopascals

$s_\infty/a_\infty = 0.74$; $\theta = 47.5^\circ$

INFLUENCE OF PRIMARY NOZZLE POSITION
ON EJECTOR PERFORMANCE
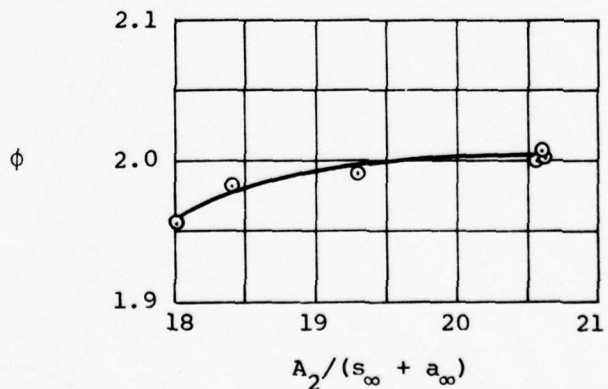
$\xi = 12.5$ cm; $\eta = 2.5$ cm; $\theta = 47.5^\circ$
$P_0 = 24.1$ kilopascals

INFLUENCE OF AREA RATIO (THROAT TO INJECTED AREAS)
ON EJECTOR PERFORMANCE

CONFIGURATION A

Figure 13.   PERFORMANCE OF CONFIGURATION A EJECTOR

c. Configuration B

Reduction of the variation of maximum pressure gradient among streamlines in the corners could be accomplished by increasing b as shown on Figure 11, but this resulted in a longer diffuser and was considered undesirable.

Thus, further investigations were undertaken to attempt to find a design which reduced the difference of maximum pressure gradients with minimal increase in the length of the diffuser.

This investigation was comprised of a search, with the aid of the computer, for vortex distribution of a more complex shape, which produced a more uniform distribution of maximum pressure gradients among the streamlines, and thus a reduced peripheral pressure gradient.

The procedure followed included a variation of da, db, and dc individually and in combination, while recording the maximum pressure gradient on each streamline, the maximum length of the diffuser using the same boundary conditions described previously, and the variation of β_o among the various streamlines.

The requirements set forth for a satisfactory diffuser design were

   a) Overall maximum pressure gradient is less than that of Configuration A.

   b) Reduce the difference in maximum pressure gradients among the various streamlines to values smaller than those of Configuration A.

   c) Avoid initial flow angles (β_o) in excess of 10°.

   d) Minimize diffuser length $(z_o - z_e)_{max}$ to the extent possible and consistent with a, b, and c above. Diffuser length is determined by the streamline having the largest extent in the z direction at a given β_e. This maximum occurs in two distinct regions as can be observed on Figure 12. In that figure, the end streamline (first maximum) is the longest in the z direction; however a second maximum exists in a streamline on the side (near the corner) of the diffuser. This second maximum is, under certain conditions, larger than the first.

Retaining the middle plane conditions β_o = 9.61 degrees, β_e = 45 degrees $2x_e/X_2$ = 2.5 and using the value b = 10.160 cm calculations of the pressure distribution, length and β_o were carried out for various values of da, db, and dc, where each was varied individually and in combination. The results of these investigations are summarized on Figures 14 and 15.

Figure 14 presents a plot of the maximum pressure gradient vs maximum diffuser length, for the predominant streamline. Maximum pressure gradient and maximum length may or may not correspond to the same streamline.

Figure 15 represents the change from Configuration A of the maximum pressure gradient and of the initial angle β_o for the entire set of stream- lines originating at points around the periphery described in centimeters from the center of the end of the diffuser jet.

Increasing da by a small amount while maintaining db = dc = 0 resulted in a decrease of the maximum pressure gradient, a small decrease in the difference in pressure gradient maxima among the streamlines, a small variation in the dis- tribution of β_o and a slight increase in diffuser length compared to Configuration A as illustrated on Figures 14 and 15.

The increase in length (Figure 14) was very slight until da reached a value of 1.91 cm, where further increase caused a more rapid increase in length as a function of maximum pressure gradient. This is a result of the predominance of the faster increasing second maximum when da exceeds 1.91 cm.

Increasing db while da = dc = 0 resulted in an opposite change in diffuser length, difference in maximum pressure gradient from that resulting from a change in the quantity b itself.

While the diffuser length decreased dramatically (Figure 14), the maximum pressure gradient near the corners increased in comparison to Configuration A as illustrated on Figure 15.

Increasing dc while da = db = 0 provided a decrease in maximum pressure gradient and diffuser length as indicated on Figure 14.

The distribution of the maximum pressure gradient among the streamlines showed a decrease near the corners and an increase near the middle plane. This is a very desirable situation from the point of view of reductions of cross flow effects.

The rapid increase of β_o near the ejector end (Figure 15) seriously limits the application of dc.
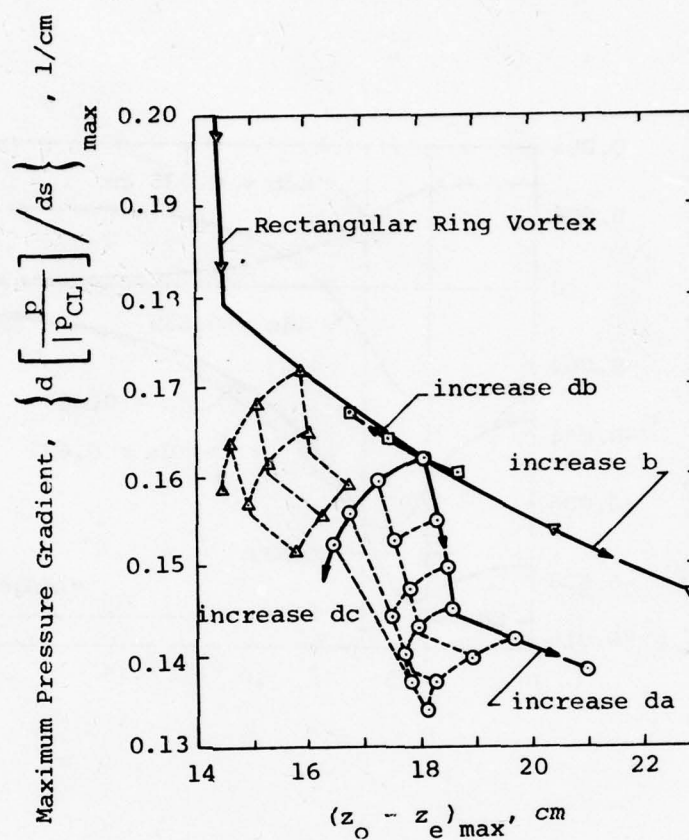
Figure 14. MAXIMUM PRESSURE GRADIENT VS MAXIMUM DIFFUSER LENGTH FOR CONSTANT DIFFUSER EXIT ANGLE
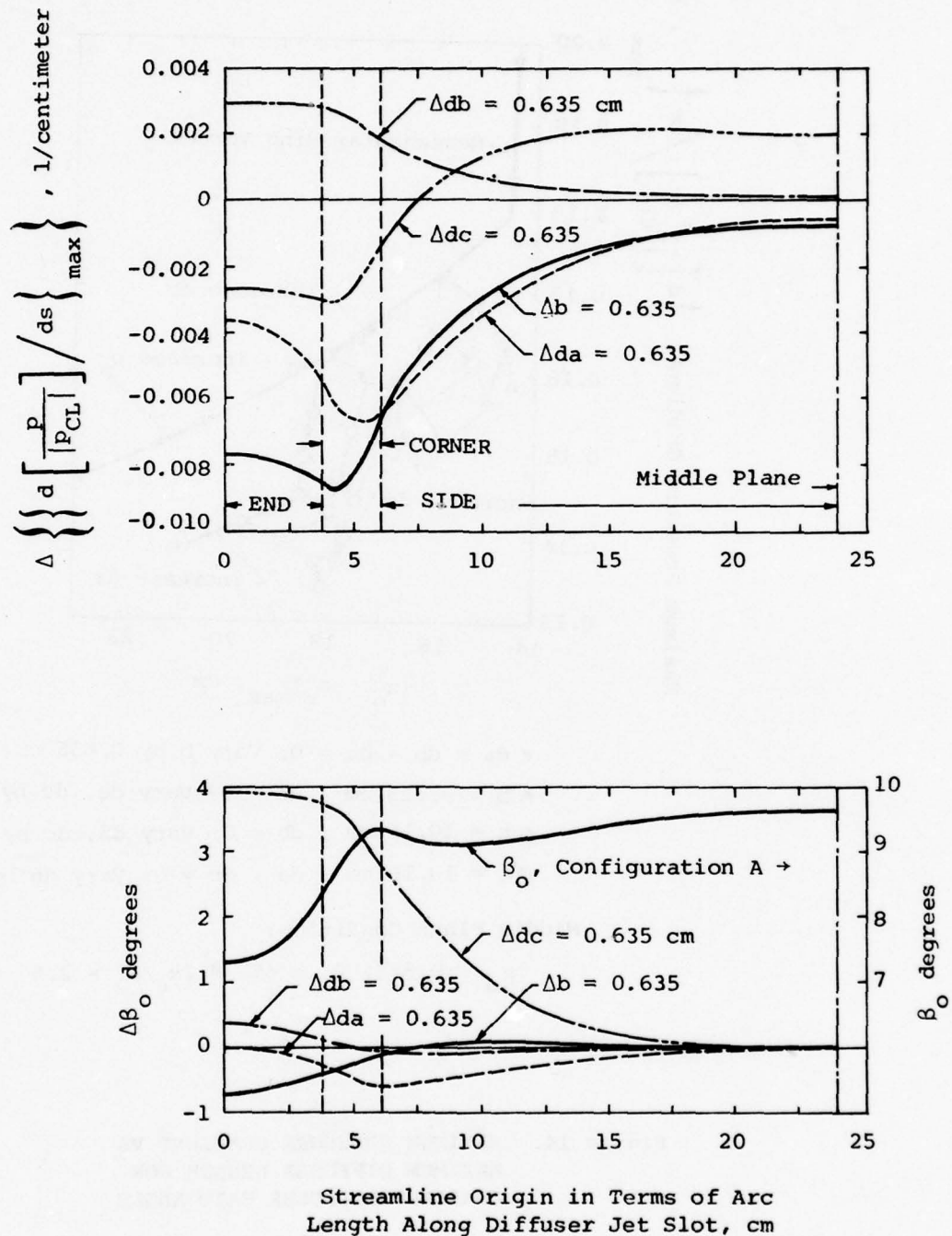
Figure 15.   VARIATION OF MAXIMUM PRESSURE GRADIENT AND INITIAL STREAMLINE
ANGLE DISTRIBUTION WITH 0.635 cm   INCREMENT OF b; da; db; and dc
ON DIFFUSER CONFIGURATION A

A repetition of these calculations for b = 9.525 cm produced the results represented by the upper network on Figure 14. The essential aspect of these results consists of the fact that the knee of the curves lies closer to da = 0. In other words, the optimal condition where the first and second maxima are equal occurs with a smaller value of da. It was therefore assumed, and later confirmed, that an increase in b, to values greater than 10.160 cm would permit larger values of da to be used before reaching the knee of the curve.

After further lengthy numerical calculations, it was determined that by a combination of an increase of b (> 10.160 cm), to take advantage of larger values of da and an increase of db, the pressure gradient could be made more uniform peripherally than that of Configuration A. In addition, increases of da and dc were combined to avoid excessive lengthening of the diffuser. Furthermore, β_e was increased to 50 degrees to shorten the diffuser length, and thus reduce skin friction. The increase of maximum pressure gradient due to increased β_e is small and is partially compensated by the decrease due to the usage of b, da, db, and dc.

Under these assumptions, the choice of

$$b = 10.795 \text{ cm}$$
$$da = 4.445 \text{ cm}$$
$$db = 0.9525 \text{ cm}$$
$$dc = 0.762 \text{ cm}$$

was made and in satisfying the middle plane requirements

$$\beta_o = 9.61 \text{ degrees}$$
$$\beta_e = 50 \text{ degrees @ } 2x_e/X_2 = 2.5$$

the values

$$a = 13.5930 \text{ cm}$$
$$c = 1.2499 \text{ cm}$$

were determined.

The maintenance of a constant value of β_e for all streamlines results in a non-uniform distribution of $(z_o - z_e)$. From a practical viewpoint, it is more desirable to terminate the diffuser at a constant value of $(z_o - z_e)$ for all streamlines. A cut-off of the Configuration A diffuser at constant $(z_o - z_e) = 13.5$ cm, thus resulting in a non-uniform distribution of β_e (Figure 16), was tested with virtually no adverse effect. Therefore a similar cut-off was performed on the above described diffuser, at $z_o - z_e = 12.7$ cm. The cut-off diffuser, labelled Configuration B, having the characteristics shown on Figure 16 in comparison to the characteristics of the cut-off Configuration A with $(z_o - z_e) = 13.5$ cm, was then fabricated and tested.

As shown on the lower curve of Figure 16, the diffuser jet slot thickness (t_d) near the corner was enlarged to achieve reasonable uniformity of the diffuser jet thickness at the end of the solid surface of the diffuser. The requirement for a larger t_d near the corner is related to the larger surface divergence and higher maximum pressure gradient for stream tubes near the corner.

As shown on Figure 16, the angle β_e is considerably smaller than 45 degrees near the ends and at the corners of the ejector. This might result in a penalty in performance of the diffuser jet.

The resulting shape of Configuration B is shown on Figure 17 by contour lines at 1.27 cm spacing and streamlines of the diffuser and a side view showing the constant $(z_o - z_e)$ cut-off. The entire ejector assembly with diffuser Configuration B is presented in Figure 4.

The performance of this ejector, as a function of the position and orientation of the primary nozzles, is shown on Figure 18. The thrust augmentation of this ejector, with the cut-off diffuser having a length of 12.7 cm, exceeded 2.13 at the optimal setting of the primary nozzles and with an area ratio $A_2/(s_\infty + a_\infty)$ of 21. Tests at smaller values of s_∞/a_∞ are desirable but would require design of a shorter diffuser to avoid excessive skin friction. This is possible since the present Configuration B has a maximum pressure gradient which is only about 80% of the maximum pressure gradient of the STAMP AJDE.
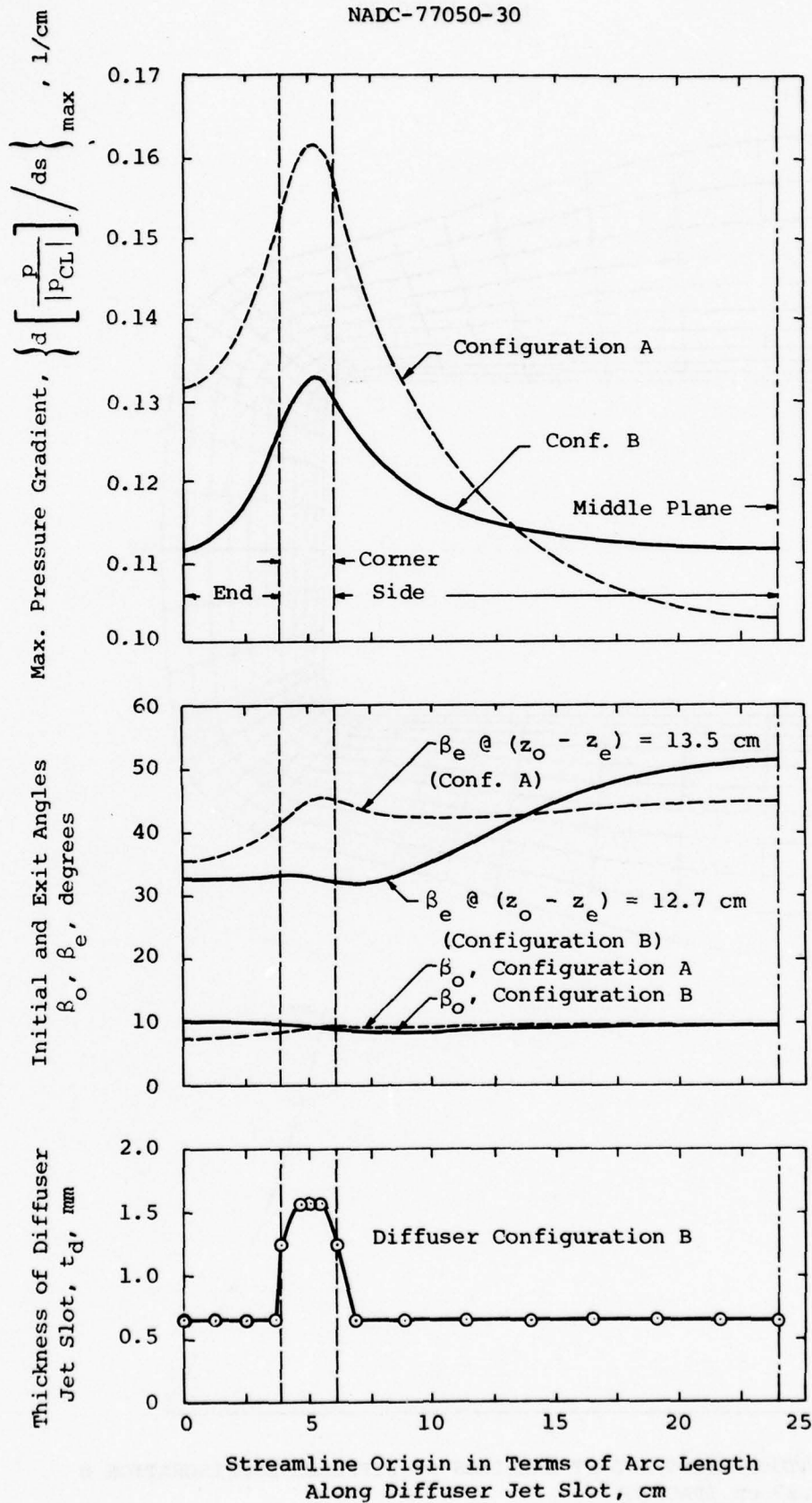
Figure 16. COMPARISON OF CONFIGURATIONS A AND B
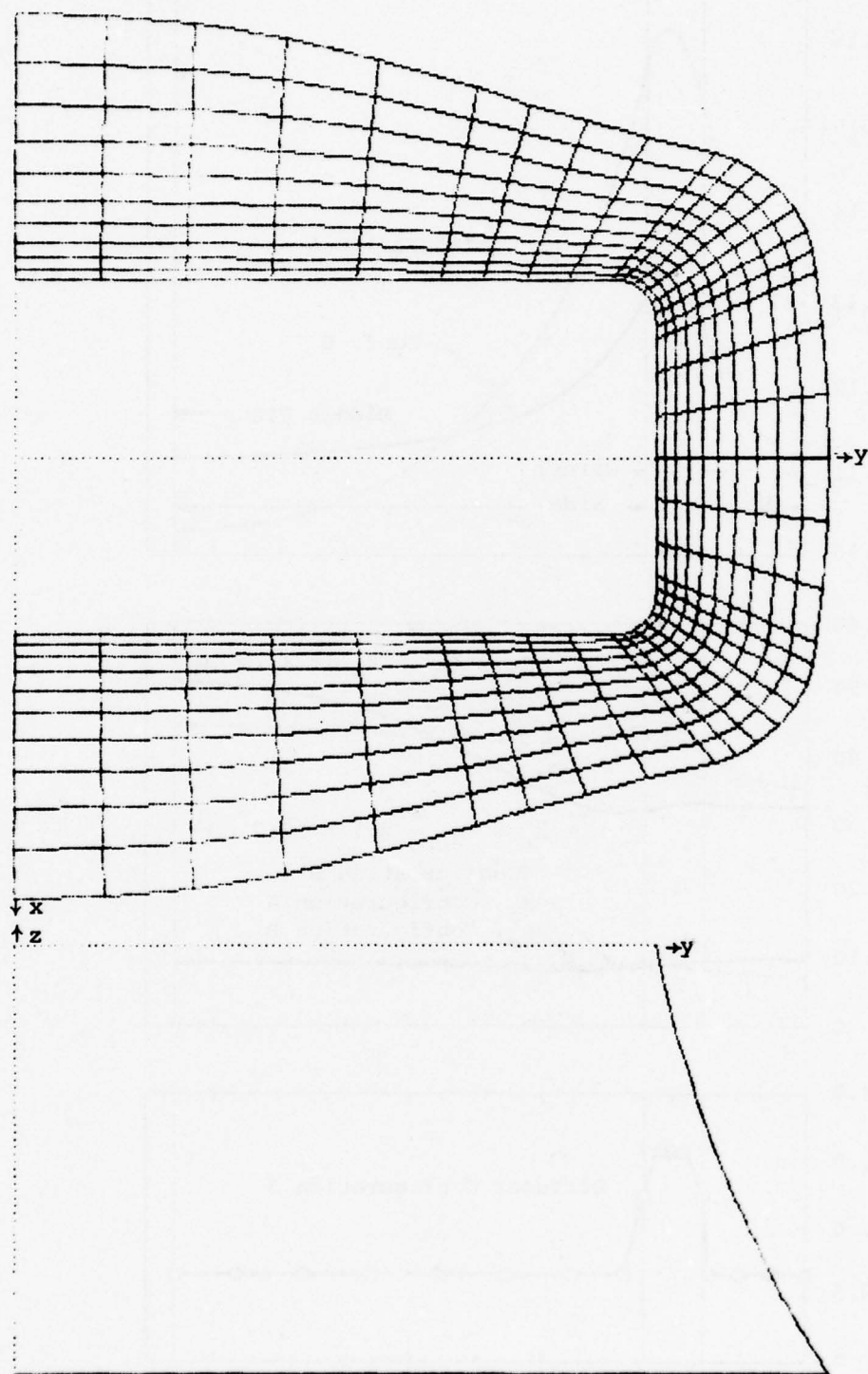
CONTOUR LINES AND STREAMLINES OF DIFFUSER CONFIGURATION B
(1.27 cm SPACING)

Figure 17.   DIFFUSER CONFIGURATION B
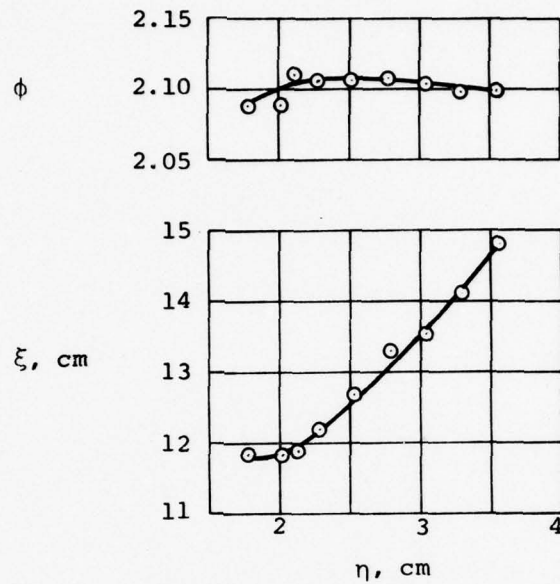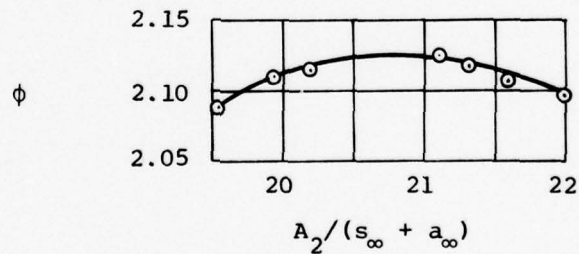
Figure 18.   CONFIGURATION B PERFORMANCE

IV   GROUND EFFECTS

The influence of ground plane proximity to the ejector's exit plane on thrust augmentation is of importance for V/STOL applications of ejector thrusters.

Since it appears likely that the influence of the ground plane is related to its influence upon the flow pattern within and around the ejector, and the effectiveness of the diffuser in particular, some limited investigations were carried out during the series of tests reported herein.

This test set-up utilized a large 2.74 m x 3.05 m flat plate which could be moved with respect to the ejector, to vary its distance from the exit plane of the ejector.

The thrust augmentation of the STAMP and Configuration B ejectors were measured over a range of distances from 0.5 to 5 meters between ejector exit plane to ground plane.

As indicated on Figure 19, the thrust augmentation of Configuration B decreased less than 2% (from 2.1 to 2.05) over most of the range of distances until the ejector was within 0.75 m from the ground plane. As the distance decreased to values smaller than 0.75 m, the mean thrust dropped rapidly. Preliminary observation of the Configuration B ejector when the ground plane is at 0.56 m from its exit indicates that the flow within the ejector duct and near the diffuser exit is free from abnormality while violent unstable flow is developed on and near the ground plane.

The thrust augmentation of the STAMP ejector decreased by about 4% (from 2.05 to 1.95) over most of the range of distances and its rapid drop at about 0.75 m was more severe than that of the Configuration B ejector, as indicated on Figure 19.

The decrease in thrust augmentation with distances smaller than 0.75 m was more pronounced for the equivalent STAMP Ejector with semi-circular end plates than for the Configuration B ejector, as shown on Figure 19. This indicates that the Configuration B is a more stable ejector than the STAMP ejector.

This effect may depend upon the ejector's stagnation pressure and upon its geometric arrangement, but more detailed tests were beyond the scope of the present investigation.
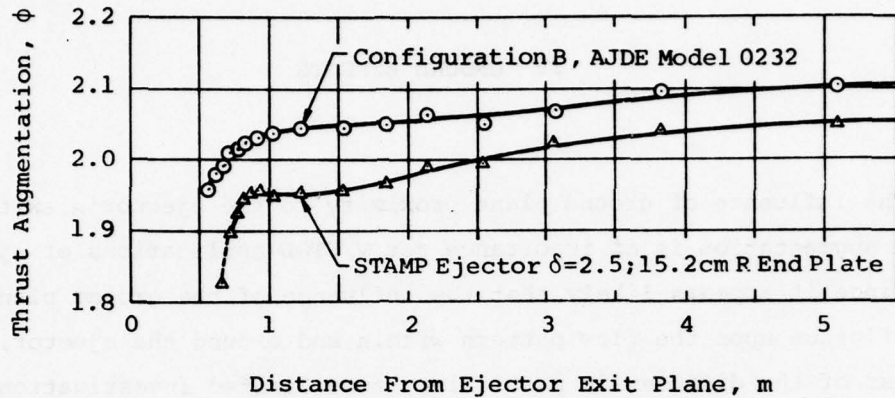
Figure 19.   INFLUENCE OF GROUND PLANE ON EJECTOR PERFORMANCE
(see Figures 1 and 4 for ejector dimensions)

V CONCLUSIONS AND REMARKS

The successful elimination of the large, protruding semi-circular end plates used on the STAMP Ejector, accompanied by a gain in performance, demonstrates the utility of potential flow methods for the design of ejector surface shapes.

Application of the potential flow methods to ejector design however, requires careful attention to a number of factors which are important from the viewpoint of real fluid phenomena. These factors can only be observed by experimental techniques in which each is carefully controlled.

Examples of these types of considerations include:

1. The avoidance of excessive discontinuities in flow direction, such as the distribution of β_o, as discussed;

2. The avoidance of cross-flow in the ejector, which can result from

   a. Peripheral pressure gradients

   b. Non-uniform distribution of boundary layer control blowing;

3. Excessive diffuser length and the accompanying skin friction loss.

The investigations of various vortex distributions and the determination of the influence of changes in the shape of the ring vortex upon the flow is extremely time consuming, but the information obtained during this effort provided a guide to the achievement of acceptable pressure gradients and diffuser lengths. The Configuration B ejector which was fabricated and tested was a result of these considerations, and its superior performance while eliminating the large, protruding end plates used on the STAMP Ejector, confirm the utility of the design procedure.

The design of the diffuser using potential flow methods also improved the stability of the flow as indicated by the reported ground effect tests. These tests performed with the Configuration B and the STAMP Ejectors in similar geometric arrangements indicated that the adverse effect of ground proximity on the Configuration B Ejector was about one-half as large as that on the STAMP Ejector. This is believed to be a direct result of the elimination of the flat, non-diverging ends which were required on the STAMP Ejector, in favor of the active, diverging, ends designed by the method described in this document and used on Configuration B.

VI REFERENCES

1. Alperin, M., Wu, J. J., and Smith, Ch. A., "The Alperin Jet-Diffuser Ejector (AJDE) Development, Testing and Performance Verification Report," February 1976, NWC TP 5853.

2. Prandtl, L. and Tiejens, "Fundamentals of Hydro- and Aeromechanics," Dover Publications, Inc. New York, New York, 1934.

3. Milne-Thomson, L. M., "Theoretical Aerodynamics," 3rd Edition, MacMillan Co., London, 1958.

APPENDIX A

TEST EQUIPMENT

The FDRC Static Test Rig is comprised of a floating structure, a 50 HP Roots Connersville Compressor and Motor, load cells for force measurement and transducers for the measurement of pressures and temperatures.

The floating structure, shown on Figure A-1, is supported by three ball supports and two flexible bellows through which the compressed air is supplied to the distribution box as illustrated.

Air is supplied to the primary nozzles and the diffuser jet nozzles through separated, metered ducts and valves which are remotely controlled from the console. A by-pass line (not shown) with a remotely controlled valve is used to adjust the mass flow to the distribution box and ejector.

Forces on the ejector are transmitted through the floating structure to the load cells, and converted to a digital readout by signal conditioners at the console.

Similarly, pressure and temperature transducers transmit their signals to conditioners which then transmit their signals to a digital readout at the console.

The test rig is carefully calibrated, to provide corrections for tare forces introduced by the bellows over the range of pressures and temperatures encountered. These corrections are applied to the readings of the forces through a computer program which provides the necessary force, mass flows and flow velocities and determines the ejector performance in terms of thrust augmentation.

Additional details of test equipment are presented in Reference 1.

Valve
Assembly

Orifice

Thrust Line
Load Cell

Ball Support

Air Distribution Box

Side Force Load Cell

Ball Support

Compressor

Orifice

Valve
Assembly

Thrust Line
Load Cell

Ball Support
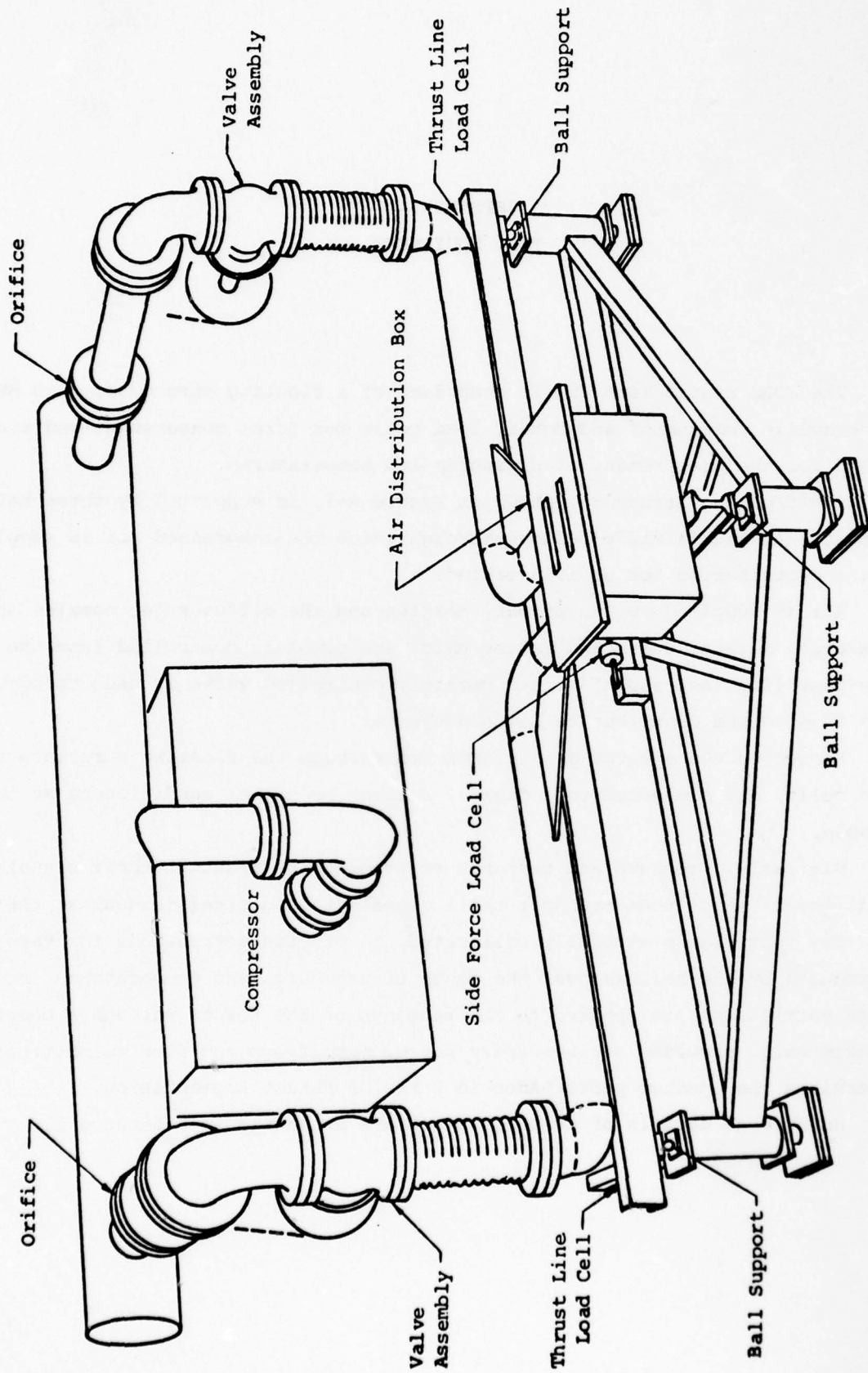
Figure A-1. FDRC Static Ejector Test Rig

APPENDIX B

COMPUTER PROGRAMS

The program for determination of the flow characteristics corresponding to any given selection of vortex distribution, described in Figure 8, is written in APL for the IBM 5100 computer, with a minimum of 32K bytes of memory.

It is comprised of 3 parts:

1. Given the quantities b, da, db, dc, and the vortex arrangement, specified by the symbol KEY, this part of the program determines a and c which satisfy the given boundary conditions at the middle plane of the ejector.

2. The main program utilized the data provided by the first part to calculate the streamline coordinates, pressures, pressure gradients, and flow angle.

3. The service programs determine the diffuser shape using the output of Part 2 and, if desired, plots this shape.

PART I FIND a AND c

Program Symbols	Written Symbols	Meaning
A,B,C DA,DB,DC	a,b,c, da,db,dc	See Figure 8
BS	b	Array of b (input)
BETA	β_e	See Figure 8
BTA	β	Flow angle with respect to thrust direction
BTAO	β_o	See Figure 8
D		Character matrix to display results
DS		Input matrix of (da, db, dc, KEY)
DELTA	δ	= $(2x_e$ @ middle plane)$/X_2$
E,F,G,H $\underline{E},\underline{F},\underline{G},\underline{H}$ EF,GH	E,F,G,H $\underline{E},\underline{F},\underline{G},\underline{H}$ EF,GH	See Figure 8
KEY		= 0 4-point vortex (E,F,G,H)
		= 1 6-point vortex (E,EF,F,G,GH,H)
		= 2 8-point vortex (E,F,$\underline{F}$,$\underline{G}$,G,H,$\underline{H}$,$\underline{E}$)
		= 3 10-point vortex (E,EF,F,$\underline{F}$,$\underline{G}$,G,GH,H,$\underline{H}$,$\underline{E}$)
		> 3 c = 0 (neglect β_o); KEY = remainder of KEY divided by 4
L	L	See Figure 8
V	$\vec{V}/\Gamma$	= (u,v,w), velocity vector, 1/cm
VN	$\vec{V}/w\Gamma$	= (u/w,v/w,1) = ($\Delta x/\Delta z,\Delta y/\Delta z,1$)
X	X	= (x,y,z), space vector
XE	x_e	See Figure 8
XN	$\vec{x}_e$	= (x_e,y_e,z_e)
XO	$\vec{x}_o$	= (x_o,y_o,z_o)
X2	X_2	See Figure 8

NOTE:
Length in centimeters.

```
      ⎕LX←'ABSTRACT'
      ⎕PW←74


    ∇ ABSTRACT
[1]   XO← 5.334 19.05 ¯1.6256
[2]   A←13.6
[3]   X2←10.16
[4]   L←38.1
[5]   BTAO←0.1677
[6]   BETA←○÷3.6
[7]   DELTA←2.5
[8]   ΔZ←¯0.254
[9]   DETOUR←1
[10]  MODEL←'AJDE MODEL 0232 DIFFUSER CONFIGURATION '
[11]  CONF←'B'
[12]  3⍴⎕AV[157]
[13]  'PROJECT:',MODEL,CONF
[14]  'ABSTRACT: A C = F(B,DA,DB,DC) FOR 10-POINT VORTEX'
[15]  '          UNLESS OTHERWISE SPECIFIED, ASSUME:'
[16]  '          STREAMLINE START AT, XO=( ',(⍕XO),' )'
[17]  '              WITH ANGLE, BTAO=',(⍕BTAO×180÷○1),' DEG.'
[18]  '          EJECTOR THROAT, X2=',(⍕X2),', L=',⍕L
[19]  '          DIFFUSER: DELTA=',(⍕DELTA),', BETA=',(⍕BETA×180÷○1),' DEG.'
[20]  '          INITIAL TRIAL VALUE FOR A, A=',⍕A
[21]  '          INTEGRATION INCREMENT, ΔZ=',⍕ΔZ
[22]  '          DETOUR=1 TO CONTINUE INDEX IB;IDA'
[23]  'SYNTAX: BS FIND A          EXAMPLE: 10 FIND A'
[24]  'NOTES:  1. BS CAN BE A NUMERIC ARRAY.'
[25]  '        2. TYPE ''D'' TO DISPLAY OUTPUT (ANY TIME)'
[26]  '           FLIGHT DYNAMICS RESEARCH CORP. 1978'
    ∇
```

```
      ∇ R←BS FIND A
[1]    XE←DELTA×X2÷2
[2]    K←5,0,8,4,8,4,7,4,7,4,7,4,7,4,6,2,6,2,7,2,6,2
[3]    R←ι0
[4]    →(DETOUR=1)/DALOOP
[5]    IB←1
[6]    T←'  ID#    A        B        C       DA       DB       DC       XE'
[7]    T←T,'    YE       ZE     BETA'
[8]    D←(1 74 ρ' '),[1](1 74 ρ(74↑T)),[1](1 74 ρ' ')
[9]    D←(1 74 ρ(74↑(16ρ' '),MODEL,CONF,'--ID#')),[1] D
[10]   BLOOP:IDA←1
[11]   DALOOP:B←(,BS)[IB]
[12]   IDN←⌊0.5+((B-5.715),(DA←DS[IDA;1]),(DB←DS[IDA;2]),DC←DS[IDA;3])÷0.635
[13]   IDN←10⊥IDN,KEY←DS[IDA;4]
[14]   KEY←4|KEY+0×NOC←KEY>3
[15]   AA←A
[16]   ΔA←0
[17]   FA1←0
[18]   C←0
[19]   N←¯1
[20]   ITERATION:N←N+1
[21]   X←X0
[22]   FA←FA1
[23]   AA←AA+ΔA
[24]   ΔC←0
[25]   FC1←0
[26]   M←¯1
[27]   CΔΔ:M←M+1
[28]   C←C+ΔC
[29]   FC←FC1
[30]   E←(AA+2×DA),(-B+DB),C+2×DC×1≠KEY
[31]   F←(-AA+2×DA),(-B+DB),C+2×DC×1≠KEY
[32]   G←(-AA+2×DA),(L+B+DB),C+2×DC×1≠KEY
[33]   H←(AA+2×DA),(L+B+DB),C+2×DC×1≠KEY
[34]   EF←0,(-B-DB),C+2×DC×(1=KEY)+(1≠KEY)×(B-DB-X2÷2)÷(B+DB+X2÷2)
[35]   G←(0,(L-X2),0)+F←(-AA),(X2÷2),C
[36]   GH←0,(L+B-DB),C+2×DC×(1=KEY)+(1≠KEY)×(B-DB-X2÷2)÷(B+DB+X2÷2)
[37]   H←(0,(L-X2),0)+E←AA,(X2÷2),C
[38]   →NOC/INTEGRATION
[39]   V←X VELOCITY KEY
[40]   BTA←¯3○(+/(2↑V÷V[3])*2)*0.5
[41]   ΔC←((M=0)×0.1)+(M≠0)×ΔC×FC1÷(FC-FC1←BTA-BTAO)
[42]   →((0.0001)<|ΔC)/CΔΔ
[43]   INTEGRATION:V←X VELOCITY KEY
[44]   XN←X+ΔZ×VN←V÷V[3]
[45]   →(XN[1]≥XE)/OVERSHOOT
[46]   →INTEGRATION,ρX←XN
[47]   OVERSHOOT:XN←X+VN×(XE-X[1])÷VN[1]
[48]   V←XN VELOCITY KEY
[49]   BTA←¯3○(+/(2↑V÷V[3])*2)*0.5
[50]   ΔA←((N=0)×0.1)+(N≠0)×ΔA×FA1÷(FA-FA1←BTA-BETA)
[51]   →((0.0001)<|ΔA)/ITERATION
[52]   D←D,[1](1 74 ρ(K⊤IDN,AA,B,C,DA,DB,DC,XN,BTA×180÷○1))
[53]   R←R,A←AA
[54]   →((1↑ρDS)≥IDA←IDA+1)/DALOOP
[55]   →((ρ,BS)≥IB←IB+1)/BLOOP
[56]   []←D
[57]   →0,ρ[]←5ρ[]AV[157]
      ∇
```

```
      ∇ R←X VELOCITY KEY
[1]     →KEYΦP4,P6,P8,P10
[2]    P4:→0,R←(X VEL E,F)+(X VEL F,G)+(X VEL G,H)+X VEL H,E
[3]    P6:R←(X VEL E,EF)+(X VEL EF,F)+(X VEL F,G)+X VEL G,GH
[4]     →0,R←R+(X VEL GH,H)+X VEL H,E
[5]    P8:R←(X VEL E,F)+(X VEL F,F̲)+(X VEL F̲,G)+X VEL G,G
[6]     →0,R←R+(X VEL G̲,H)+(X VEL H̲,H)+(X VEL H̲,E)+X VEL E̲,E
[7]    P10:R←(X VEL E,EF)+(X VEL EF,F̲)+(X VEL F̲,F̲)+(X VEL F̲,G)+X VEL G,G
[8]     →0,R←R+(X VEL G̲,GH)+(X VEL GH,H)+(X VEL H̲,H̲)+(X VEL H̲,E̲)+X VEL E̲,E
      ∇


      ∇ V←P VEL AB;A;B;AP;BP;AAP;UAB;UAP;UBP;Q
[1]  ⍝ VELOCITY PER UNIT Γ AT P CAUSED BY A LINE VORTEX SPANED FROM A TO B
[2]  ⍝ SYNTAX: (XP,YP,ZP) VEL (XA,YA,ZA),(XB,YB,ZB)
[3]     →(((ρρP)≠1)∨((ρρAB)≠1)∨((ρP)≠3)∨((ρAB)≠6))/ERR
[4]     UAP←AP÷AAP←(+/(AP←P-A←3↑AB)*2)*0.5
[5]     UBP←BP÷(+/(BP←P-B←3↓AB)*2)*0.5
[6]     Q←(UAB←AB÷(+/(AB←B-A)*2)*0.5) CROSS UAP
[7]     →0,V←Q×((+/UAB×UAP)-+/UAB×UBP)÷○4×AAP×((+/Q×Q)+((+/Q×Q)=0))
[8]   ERR:→0,ρ⎕←'ARGUMENT ERROR IN VELOCITY FUNCTION'
      ∇


      ∇ C←A CROSS B
[1]  ⍝ VECTOR PRODUCT C = A × B
[2]     →(((ρρA)≠1)∨((ρρB)≠1)∨((ρA)≠3)∨((ρB)≠3))/ERR
[3]     →0,C←((1ΦA)×(2ΦB))-(2ΦA)×(1ΦB)
[4]   ERR:→0,ρ⎕←'ARGUMENT ERROR IN CROSS FUNCTION'
      ∇
```

SAMPLE INPUT

```
DETOUR←0
BS←10.795
DS←1 4ρ4.445,0.9525,0.762,3
```

BS FIND A

SAMPLE OUTPUT

AJDE MODEL 0232 DIFFUSER CONFIGURATION B-ID#

ID#	A	B	C	DA	DB	DC	XE	YE	ZE	BETA
87213	13.5932	10.7950	1.2499	4.4450	.9525	.7620	12.70	19.05	¯13.93	50.00

PART II MAIN PROGRAM

Program Symbols	Written Symbols	Meaning
A,B,C da,db,dc	a,b,c da,db,dc	See Figure 8
BETA	β_e	Maximum exit β for all streamlines
BTA	β	Flow angle with respect to thrust direction
CONF		Configuration (1 to 3 characters)
CUT		Maximum -z for all streamlines
E,F,G,H E,F,G,H EF,GH	E,F,G,H E,F,G,H EF,GH	See Figure 8
FILE		File number of the tape
KEY		= 0 4-point vortex (E,F,G,H)
		= 1 6-point vortex (E,EF,F,G,GH,H)
		= 2 8-point vortex (E,F,F,G,G,H,H,E)
		= 3 10-point vortex (E,EF,F,F,G,G,GH,H,H,E)
		> 3 c = 0; KEY = remainder of KEY divided by 4
K1,K2,K3,K4		Constants
L	L	See Figure 8
MODEL		Ejector model
P	p	Normalized pressure, $-(\text{pressure})/p_{CL}$
PCL	$-p_{CL}/\Gamma^2$	$= u^2 + v^2 + w^2$ @ center of the ejector, $1/cm^2$
S	s	Streamline coordinate, cm
V	$\vec{V}/\Gamma$	$= (u,v,w)$ velocity vector, $1/cm$
VN	$\vec{V}/w\Gamma$	$= (u/w,v/w,1) = (\Delta x/\Delta y, \Delta y/\Delta z, 1)$
X	$\vec{x}$	$= (x,y,z)$, space vector
Δ		Integer matrix for data storage
		First row = K1 x $(a,b,c,-p_{CL},\text{ID \#},\text{streamline \#},\text{Conf. \#})$
		Second row = 10^8 x $(da,db,dc,0,0,0,0,)$
		Other row = 10^8 x $(x,y,z,\beta,s,p/p_{CL},d(p/|p_{CL}|)/ds)$
$\underline{A}$		Table of $(a,b,c,da,db,dc,\text{KEY})$ combination
$\underline{X}$		Table of streamline origin $(x_o,y_o,z_o,\text{streamline \#})$
		Or, optional $(x_o,y_o,z_o,\text{streamline \#, Maximum -z})$

NOTES:
1. Last column of the output is $d(p/|p_{CL}|)/ds$
2. Length in centimeters

```
      □LX←'ABSTRACT'
      □PW←80




    ∇ ABSTRACT
[1]    K1←(3ρ100000000),10000000000,(3ρ1)
[2]    K2←1,1,1,(180÷○1),1,1,1
[3]    K3←(6ρ 9 4),9,3,(6ρ 9 4)
[4]    K4←100000000
[5]    X2←10.16
[6]    L←38.1
[7]    BETA←○÷3
[8]    ΔZ←¯0.254
[9]    CUT←14.3256
[10]   MODEL←' AJDE MODEL 0232 DIFFUSER CONFIGURATION '
[11]   CONF←'B'
[12]   □←3ρ□AV[157]
[13]   'PROJECT:',MODEL,CONF
[14]   'ABSTRACT: DIFFUSER SHAPE, PRESSURE DISTRIBUTION AND GRADIENT'
[15]   '    CONFIGURATION PARAMETERS:'
[16]   '    X2 = ',(⍕X2),';    L = ',(⍕L),'; MAX BETA = ',(⍕BETA×K2[4]),' DEG.'
[17]   '    INTEGRATION INCREMENT, ΔZ = ',(⍕ΔZ),';   MAX -ZE = ',⍕CUT
[18]   '    STREAMLINE ORIGIN: X ( ',(⍕ρX),' MATRIX)'
[19]   '    A B C RELATION:    Ā ( ',(⍕ρÂ),' MATRIX)'
[20]   'CALCULATION: TYPE ''RUN̄ N1'', OR, ''RUN N1 TO N2'''
[21]   '    N1, N2 = ((ROW OF A) - 1) × ',(⍕1↑ρX),' + (ROW OF X̲)'
[22]   'PLAYBACK: TYPE ''PLAYB̄ACK FILE# FROM M̄1 TO M2'''
[23]   '    OR, ''PLAYBACK FILE#'', OR, ''PLAYBACK FILE# FROM M1'''
[24]   'PRINT: TYPE ''PRINT'', OR ''PLAYBACK 0'''
[25]   '                    FLIGHT DYNAMICS RESEARCH CORP. 1978'
    ∇
```

```
      ∇ RUN NUMBER
[1]    ⍝ NUMBER = DECODE VALUE OF ROW NUMBERS OF MATRIX A AND X
[2]    ⍝ SINGLE RUN, TYPE 'RUN N1'; MULTIPLE RUN TYPE 'RUN N1 T̄O N2'
[3]     WRONG←'INVALID RUN NUMBER, TRY AGAIN'
[4]     DUMMY←(FILE←0),(N←(,NUMBER)[1])
[5]     →(1=ρ,NUMBER)/PROCEED
[6]     →((N2←(,NUMBER)[2])≥(N1←N))/(⎕LC[1]+2)
[7]     →0,0ρ⎕←WRONG
[8]     CASES←1+N2-N1
[9]     N←N1+(⍳CASES)-1
[10]  PROCEED:N←((N>0)∧(N≤(1↑,ρA)×(1↑,ρX̲)))/N
[11]    →(0<CASES←ρ,N)/(⎕LC[1]+2̄)
[12]    →0,0ρ⎕←WRONG
[13]    I←1+0×ρρ⎕←' '
[14]  QX:'DO YOU WISH TO EXPUNGE SOME FUNCTIONS TO CONSERVE WS (0=N, 1=Y)'
[15]    →(2 1 +.× 0 1 =1↑,⎕)⌽QX,EX,Q
[16]  EX:X←⎕EX 4 8 ρ'ABSTRACTPLAYBACKSUMMARY FROM    '
[17]  Q:⎕←'DO YOU WISH TO RECORD RESULTS ON TAPE (0=N  1=Y)'
[18]    →(2 1 +.× 0 1 =1↑,⎕)⌽Q,YES,NO
[19]  YES:⎕←'ENSURE OUTPUT DATA TAPE IS ON, AND MARKED'
[20]    DUMMY←⍞,0ρ⎕←'HIT EXECUTE KEY TO CONTINUE'
[21]    →(0≥FILE←1↑,⍞,0ρ⎕←'ENTER OUTPUT FILE NUMBER')/⎕LC[1]
[22]  RE:'DO YOU WISH TO RECORD FROM THE BEGINNING OF THE FILE (0=N, 1=Y)'
[23]    →(∧/ 0 1 ≠NEW←1↑,⍞)⌽REPEAT,RE
[24]  NO:DUMMY←⍞,0ρ⎕←'ENSURE PRINTER IS ''ON'', HIT EXECUTE TO CONTINUE'
[25]  REPEAT:M←,1+(10,(1↑,ρA),(1↑,ρX̲))⊤(,,N)[I]-1
[26]    →(⎕LC[1]+1),(A←A[M[2];1]),(B←A[M[2];2]),(C←A[M[2];3]),DC←A[M[2];6]
[27]    IDN←⌊0.5+((B-5.7̄15),(DA←A[M[2̄];4]),(DB←A[M[2̄];5]),DC)÷0.6̄35
[28]    IDN←10⊥IDN,KEY←A[M[2];7]+0×CFN←+/(100000̄0,1000,1)×⎕AV⍳3↑CONF
[29]    E←(A+2×DA),(-B+D̄B),C+2×DC×1≠KEY←4|KEY
[30]    F←(-A+2×DA),(-B+DB),C+2×DC×1≠KEY
[31]    G←(-A+2×DA),(L+B+DB),C+2×DC×1≠KEY
[32]    H←(A+2×DA),(L+B+DB),C+2×DC×1≠KEY
[33]    EF←0,(-B-DB),C+2×DC×(1=KEY)+(1≠KEY)×(B-DB-X2÷2)÷(B+DB+X2÷2)
[34]    G←(0,(L-X2),0)+F←(-A),(X2÷2),C
[35]    ḠH←0,(L+B-DB),C̄+2×DC×(1=KEY)+(1≠KEY)×(B-DB-X2÷2)÷(B+DB+X2÷2)
[36]    H←(0,(L-X2),0)+E̲←A,(X2÷2),C
[37]    X̄←0,(L÷2),0
[38]    PCL←+/(V←X VELOCITY KEY)*2
[39]    →(4≥⁻1↑,ρX)/INTEGRATION,(X←X[M[3];⍳3]),(S←0),(J←1),ZMX←CUT
[40]    ZMX←CUT⌊Z̄M̄X←(ZMX×0<ZMX)+CUT×0≥ZMX←X̲[M[3];5]
[41]  INTEGRATION:V←X VELOCITY KEY
[42]    →(((BETA≤BTA←⁻3○(+/(2↑VN←V÷V[3])*2)*0.5)∨(ZMX≤|X[3]))/OVER
[43]    VM←VN
[44]    D← 1 7 ρ(X,BTA,S,(P←(+/V*2)÷PCL),0)
[45]    →(J≠1)/(⎕LC[1]+2)
[46]    →⎕LC[1]+2+0×ρρ∆←D
[47]    ∆←∆,[1] D
[48]    →INTEGRATION,(0ρX←X+∆Z×VN),(0ρS←S+|∆Z×(+/VN*2)*0.5),0ρJ←J+1
[49]  OVER:→(ZMX≤|X[3])/DONE
[50]    J←J-1
```

```apl
[51]    FZO←BETA-Δ[J;4]
[52]    ΔΔZ←(ΔZ1+ΔZ)×FZ1÷FZO-FZ1←BETA-BTA
[53] ITERATION:ΔZ1←ΔZ1+ΔΔZ
[54]    FZO←FZ1
[55]    X←Δ[J;ι3]+VM×ΔZ1
[56]    V←X VELOCITY KEY
[57]    BTA←¯3○(+/(2↑V÷V[3])*2)*0.5
[58]    ΔΔZ←ΔΔZ×FZ1÷FZO-FZ1←BETA-BTA
[59]    →((1E¯6)<|ΔΔZ)/ITERATION
[60]    S←Δ[J;5]+|ΔZ1×(+/VM*2)*0.5
[61] DONE:Δ←Δ,[1](1 7 ρX,BTA,S,(P←(+/V*2)÷PCL),0)
[62]    →(3>JM←(1↑,ρΔ)-1+0×J←2)/SETTLE
[63] DIFFERENTIATION:DF3←Δ[(J+1);5]-Δ[(J-1);5]
[64]    DF1←(Δ[(J-1);6]-Δ[J;6])÷(Δ[J;5]-Δ[(J-1);5])×DF3
[65]    DF2←(Δ[J;6]-Δ[(J+1);6])÷(Δ[(J+1);5]-Δ[J;5])×DF3
[66]    →((J≠2)∧(J≠JM))/(□LC[1]+4)
[67]    →(J=JM)/(□LC[1]+2)
[68]    →□LC[1]+2+0×ρρΔ[1;7]←((DF3+Δ[2;5]-Δ[1;5])×DF1)+(Δ[1;5]-Δ[2;5])×DF2
[69]    Δ[(J+1);7]←((Δ[J;5]-Δ[(J+1);5])×DF1)+(DF3+Δ[(J+1);5]-Δ[J;5])×DF2
[70]    Δ[J;7]←((Δ[(J+1);5]-Δ[J;5])×DF1)+(Δ[J;5]-Δ[(J-1);5])×DF2
[71]    →(JM≥J←J+1)/DIFFERENTIATION
[72] ⍝ FIND MAXIMUM PRESSURE GRADIENT BY LEAST SQUARE PARABOLIC FIT
[73] ⍝ OF 3 TO 5 POINTS NEAR THE MAXIMUM
[74]    J←1↑⍒,Δ[;7]
[75]    →(3>ρZI←(ZI∊ιJM)/ZI←ZI-+/(JM←1↑,ρΔ)<ZI←((J-3)×J>2)+ι5)/SETTLE
[76]    XI←Δ[ZI;5]
[77]    YI←Δ[ZI;7]
[78]    CI←(ρ,XI),(+/,XI),(+/(,XI)*2),(+/(,XI)*3),(+/(,XI)*4)
[79]    BI←(+/,YI),(+/(,XI)×(,YI)),(+/((,XI)*2)×(,YI))
[80]    CI←,BI⌹(3 3 ρ(3↑CI),(3↑1ΦCI),(¯3↑CI))
[81]    XM←-CI[2]÷2×CI[3]
[82]    YM←+/CI×(1,XM,XM*2)
[83]    →(~((JX←¯1↑((XM≥XI)/ZI))∊ZI))/SETTLE
[84]    ΔJ←(XM-Δ[JX;5])÷(Δ[(JX+1);5]-Δ[JX;5])
[85]    INSERT←,(ΔJ×Δ[(JX+1);])+(1-ΔJ)×Δ[JX;]
[86]    INSERT[5]←XM
[87]    INSERT[7]←YM
[88]    INSERT← 1 7 ρINSERT
[89]    INSERT←⌊0.5+K4×INSERT
[90]    Δ←⌊0.5+K4×Δ
[91]    Δ←((JX,7)↑Δ),[1] INSERT,[1]((JX,0)↓Δ)
[92]    Δ←Δ÷K4
[93] SETTLE:Δ←(1 7 ρ7↑DA,DB,DC),[1] Δ
[94]    Δ←(1 7 ρ⌊0.5+K1×7↑(A,B,C,PCL,IDN,(,X[M[3];4]),CFN)),[1](⌊0.5+K4×Δ)
[95]    →(0=FILE)/DISPLAY
[96]    CODE←(I=1)∧(NEW=1)
[97]    →(0=RECORD FILE)/DISPLAY
[98]    →0,0ρ□←'RECORDING ERROR, RUN TERMINATED'
[99] DISPLAY:PRINT
[100]   →(CASES≥I←I+1)Φ0,REPEAT
      ∇
```

```
      ∇ R←X VELOCITY KEY
[1]      →(KEYΦP4,P6,P8,P10)
[2]   P4:→0,R←(X VEL E,F)+(X VEL F,G)+(X VEL G,H)+X VEL H,E
[3]   P6:R←(X VEL E,EF)+(X VEL EF,F)+(X VEL F,G)+X VEL G,GH
[4]     →0,R←R+(X VEL GH,H)+X VEL H,E
[5]   P8:R←(X VEL E,F)+(X VEL F,F̱)+(X VEL F̱,G)+X VEL G,G
[6]     →0,R←R+(X VEL G,H)+(X VEL H,H̱)+(X VEL H̱,E)+X VEL E̱,E
[7]   P10:R←(X VEL E,EF)+(X VEL EF,F̄)+(X VEL F̄,F̱)+(X VEL F̱,G)+X VEL G,G
[8]     →0,R←R+(X VEL G,GH)+(X VEL GH,H)+(X VEL H̱,H)+(X VEL H̱,E)+X VEL E̱,E
      ∇

      ∇ V←P VEL AB;A;B;AP;BP;AAP;UAB;UAP;UBP;Q
[1]   ⍝ VELOCITY PER UNIT Γ AT P CAUSED BY A LINE VORTEX SPANED FROM A TO B
[2]   ⍝ SYNTAX: (XP,YP,ZP) VEL (XA,YA,ZA),(XB,YB,ZB)
[3]     →(((ρρP)≠1)∨((ρρAB)≠1)∨((ρP)≠3)∨((ρAB)≠6))/ERR
[4]     UAP←AP÷AAP←(+/(AP←P-A←3↑AB)*2)*0.5
[5]     UBP←BP÷(+/(BP←P-B←3↓AB)*2)*0.5
[6]     Q←(UAB←AB÷(+/(AB←B-A)*2)*0.5) CROSS UAP
[7]     →0,V←Q×((+/UAB×UAP)-+/UAB×UBP)÷○4×AAP×((+/Q×Q)+((+/Q×Q)=0))
[8]   ERR:→0,ρ⎕←'ARGUMENT ERROR IN VELOCITY FUNCTION'
      ∇

      ∇ C←A CROSS B
[1]   ⍝ VECTOR PRODUCT C = A × B
[2]     →(((ρρA)≠1)∨((ρρB)≠1)∨((ρA)≠3)∨((ρB)≠3))/ERR
[3]     →0,C←((1ΦA)×(2ΦB))-(2ΦA)×(1ΦB)
[4]   ERR:→0,ρ⎕←'ARGUMENT ERROR IN CROSS FUNCTION'
      ∇

      ∇ R←M FROM N
[1]     R←M,N
      ∇

      ∇ R←N TO K
[1]     R←N,K
      ∇

      ∇ PRINT;SYM;RMX;LPP;PAGE;PAGES;X;Y;Z;I;J;JM;L
[1]     SYM←' *'
[2]     PAGES←1
[3]     →(53≥LPP←RMX←1↑ρΔ)/(⎕LC[1]+2)
[4]     LPP←48⌈⌈(RMX-2)÷PAGES←⌈(RMX-2)÷50
[5]     JM←2+1↑Ψ,Δ[(2↓⍳RMX);7]
[6]     X←Δ[1;]÷K1
[7]     Z←Δ[2;]÷K4
[8]     →LOOP,(PAGE←1),(J←3)
[9]   LOOP:⎕←2ρ⎕AV[157]
[10]    →(PAGES=1)/(⎕LC[1]+2)
[11]    ⎕←(52ρ' '),'PAGE ',(⍕PAGE),' OF ',(⍕PAGES),⎕AV[157]
[12]    Y←(Y≠' ')/Y←⎕AV[(3ρ1000)⊤X[7]]
[13]    ⎕←MODEL,Y,'-',(⍕X[5]),' STREAMLINE NO. ',(⍕X[6]),⎕AV[157]
[14]    Y←' A = ',(⍕X[1]),'   B = ',(⍕X[2]),'   C = ',(⍕X[3]),'   -PCL = ',⍕X[4]
[15]    ⎕←((0⌈32-⌊(ρY)÷2)ρ' '),Y
[16]    ' '
[17]    Y←'DA = ',(⍕Z[1]),'   DB = ',(⍕Z[2]),'   DC = ',(⍕Z[3])
[18]    ⎕←((0⌈32-⌊(ρY)÷2)ρ' '),Y,⎕AV[157]
[19]    ⎕←'     X          Y          Z       BETA       S        P/PCL DP/DS/PCL'
[20]    ' '
[21]    L←1
[22]    →(((RMX≥J←J+1)∧(LPP≥L←L+1)),0ρ⎕←(K3⍕K2×,Δ[J;]÷K4),SYM[1+J=JM])/⎕LC[1]
[23]    ⎕←(53+(2×PAGES=1)-L)ρ⎕AV[157]
[24]    →(PAGES≥PAGE←PAGE+1)/LOOP
[25]  STOP:→0
      ∇
```

```
    ∇ RTN←RECORD FILE
[1]   ⍝ RTN=0 FOR NORMAL RECORDING, RTN=1 IF ERROR
[2]   ⍝ CODE=1 RECORDING START AT RECORD 1, CODE=0 FOR ADDING RECORDS
[3]    RTN←0
[4]    ⎕WA←⎕EX 'OUTP'
[5]    →(2≠1 ⎕SVO 'OUTP')/ER1
[6]    OUTP←(4↑(4×CODE)⌽'ADD OUT '),(⍕FILE),' ID=(DATA) MSG=OFF'
[7]    →(1≠∧/0=OUTP)/ER2
[8]    OUTP←Δ
[9]    →(1≠∧/0=OUTP)/ER3
[10] STOP:OUTP←⍳0
[11]   →(1≠∧/0=OUTP)/ER4
[12]   →(2=⎕SVR 'OUTP')/0
[13] ER5:→OUT,⍴⎕←'RECORD: ERROR RETRACTING SHARED VARIABLE'
[14] ER1:→OUT,⍴⎕←'RECORD: ERROR ESTABLISHING SHARED VARIABLE'
[15] ER2:→OUT,⍴⎕←'RECORD: ERROR OPENING FILE ',⍕FILE
[16] ER3:→OUT,⍴⎕←'RECORD: ERROR RECORDING FILE ',⍕FILE
[17] ER4:→OUT,⍴⎕←'RECORD: ERROR CLOSING FILE ',⍕FILE
[18] OUT:→0×⍴(⎕EX 'OUTP'),(⎕SVR 'OUTP'),0⍴(RTN←1)
    ∇
    ∇ PLAYBACK MNK;I;M;N;K
[1]   ⍝ FULL SYNTAX:        'PLAYBACK FILE# FROM N1 TO N2'
[2]   ⍝ PARTIAL SYNTAX:     'PLAYBACK FILE# FROM N1 (TO END)'
[3]   ⍝                     'PLAYBACK FILE# (FROM 1 TO END)'
[4]   ⍝ FILE# = FILE NUMBER; N1, N2 ARE RECORD NUMBERS
[5]   ⍝ SPECIAL CASE: TYPE 'PLAYBACK FILE' TO DISPLAY ENTIRE CURRENT FILE
[6]    M←(,MNK)[1]
[7]    →(M>0)/(⎕LC[1]+3)
[8]    PRINT
[9]    →0
[10]   N←1
[11]   K←440
[12]   →(1=⍴,MNK)/(⎕LC[1]+4)
[13]   N←(,MNK)[2]
[14]   →(2=⍴,MNK)/(⎕LC[1]+2)
[15]   K←(,MNK)[3]
[16]   →((N≥1)∧(K≥N))/(⎕LC[1]+2)
[17]   →0,0⍴⎕←'INVALID RECORD DESCRIPTION, TRY AGAIN'
[18]   ⎕WA←⎕EX 'INPT'
[19]   →(2≠1 ⎕SVO 'INPT')/ER1
[20]   INPT←'IN ',(⍕M),' ID=(DATA) MSG=OFF'
[21]   →(1≠∧/0=INPT)/ER2
[22]   I←0
[23] READ:→(0=⍴,Δ←INPT)/ER3
[24]   →(N>I←I+1)/READ
[25]   PRINT
[26]   →(K≥I)/READ
[27] STOP:INPT←⍳0
[28]   →(1≠∧/0=INPT)/ER4
[29]   →(2=⎕SVR 'INPT')/0
[30] ER5:→OUT,⍴⎕←'PLAYBACK: ERROR RETRACTING SHARED VARIABLE'
[31] ER1:→OUT,⍴⎕←'PLAYBACK: ERROR ESTABLISHING SHARED VARIABLE'
[32] ER2:→OUT,⍴⎕←'PLAYBACK: ERROR OPENING FILE ',⍕M
[33] ER3:→OUT,⍴⎕←'PLAYBACK: END OF FILE ',⍕M
[34] ER4:→OUT,⍴⎕←'PLAYBACK: ERROR CLOSING FILE ',⍕M
[35] OUT:→0×⍴(⎕EX 'INPT'),(⎕SVR 'INPT')
    ∇
```

```
     ∇ SUMMARY MNK;I;M;N;K;J;X;Y
[1]   ⍝ FULL SYNTAX:      'SUMMARY FILE# FROM N1 TO N2'
[2]   ⍝ PARTIAL SYNTAX:  'SUMMARY FILE# FROM N1 (TO END)'
[3]   ⍝                  'SUMMARY FILE# (FROM 1 TO END)'
[4]   ⍝ FILE# = FILE NUMBER, N1, N2 ARE RECORD NUMBERS
[5]   ⍝ SPECIAL CASE: TYPE 'SUMMARY FILE' TO DISPLAY ALL MAX DP/DS IN FILE
[6]   M←(,MNK)[1]
[7]   →(M>0)/(⎕LC[1]+2)
[8]   →0
[9]   N←1
[10]  K←440
[11]  →(1=ρ,MNK)/(⎕LC[1]+4)
[12]  N←(,MNK)[2]
[13]  →(2=ρ,MNK)/(⎕LC[1]+2)
[14]  K←(,MNK)[3]
[15]  →((N≥1)∧(K≥N))/(⎕LC[1]+2)
[16]  →0,0ρ⎕←'INVALID RECORD DESCRIPTION, TRY AGAIN'
[17]  ⎕WA←⎕EX 'INPT'
[18]  →(2≠1 ⎕SVO 'INPT')/ER1
[19]  INPT←'IN ',(⍕M),' ID=(DATA) MSG=OFF'
[20]  →(1≠∧/0=INPT)/ER2
[21]  I←0
[22] READ:→(0=ρ,Δ←INPT)/ER3
[23]  →(N>I←I+1)/READ
[24]  J←1+1↑�,Δ[(1↓⍳1↑ρΔ);7]
[25]  →(1≠Δ[1;6])/CONTINUE
[26]  ⎕←(2ρ⎕AV[157]),(18ρ' '),'SUMMARY OF MAXIMUM PRESSURE GRADIENT',⎕AV[15
[27]  X←,Δ[1;]÷K1
[28]  ⎕←(13ρ' '),MODEL,((Y≠' ')/Y←⎕AV[(3ρ1000)⊤X[7]]),'-',(⍕X[5]),⎕AV[157]
[29]  Y←'   C = ',(⍕X[3]),'    -PCL = ',⍕X[4]
[30]  Y←'A = ',(⍕X[1]),'   B = ',(⍕X[2]),Y
[31]  ⎕←((0⌈36-⌊(ρY)÷2)ρ' '),Y
[32]  IDN←X[5]
[33]  ' '
[34]  X←,Δ[2;]÷K4
[35]  Y←'DA = ',(⍕X[1]),'   DB = ',(⍕X[2]),'   DC = ',(⍕X[3])
[36]  ⎕←((0⌈36-⌊(ρY)÷2)ρ' '),Y,⎕AV[157]
[37]  '    SL#        X      Y      Z    BETA    S     P/PCL  DP/DS ZO-ZE BETAE BE
[38]  ' '
[39] CONTINUE:→(IDN≠Δ[1;5])/(⎕LC[1]+2)
[40]  Y←Δ[1;6],((,Δ[J;]),((Δ[3;3],0)-(,Δ[(1↑ρΔ);3,4])×1,¯1),Δ[3;4])÷K4
[41]  ⎕←(5,0,9,2,6,2,6,2,6,2,6,2,7,4,7,4,6,2,6,2,6,2)⍕K2[1,(⍳7),1,4,4]×Y
[42]  →(K>I)/READ
[43] STOP:INPT←⍳0
[44]  →(1≠∧/0=INPT)/ER4
[45]  →(2=⎕SVR 'INPT')/0
[46] ER5:→OUT,ρ⎕←'SUMMARY: ERROR RETRACTING SHARED VARIABLE'
[47] ER1:→OUT,ρ⎕←'SUMMARY: ERROR ESTABLISHING SHARED VARIABLE'
[48] ER2:→OUT,ρ⎕←'SUMMARY: ERROR OPENING FILE ',⍕M
[49] ER3:→OUT,ρ⎕←'SUMMARY: END OF FILE ',⍕M
[50] ER4:→OUT,ρ⎕←'SUMMARY: ERROR CLOSING FILE ',⍕M
[51] OUT:→0×ρ(⎕EX 'INPT'),(⎕SVR 'INPT')
     ∇
```

```
      ∇ SUMMARY MNK;I;M;N;K;J;X;Y
[1]   ⍝ FULL SYNTAX:      'SUMMARY FILE# FROM N1 TO N2'
[2]   ⍝ PARTIAL SYNTAX: 'SUMMARY FILE# FROM N1 (TO END)'
[3]   ⍝                  'SUMMARY FILE# (FROM 1 TO END)'
[4]   ⍝ FILE# = FILE NUMBER, N1, N2 ARE RECORD NUMBERS
[5]   ⍝ SPECIAL CASE: TYPE 'SUMMARY FILE' TO DISPLAY ALL MAX DP/DS IN FILE
[6]   M←(,MNK)[1]
[7]   →(M>0)/(⎕LC[1]+2)
[8]   →0
[9]   N←1
[10]  K←440
[11]  →(1=ρ,MNK)/(⎕LC[1]+4)
[12]  N←(,MNK)[2]
[13]  →(2=ρ,MNK)/(⎕LC[1]+2)
[14]  K←(,MNK)[3]
[15]  →((N≥1)∧(K≥N))/(⎕LC[1]+2)
[16]  →0,0ρ⎕←'INVALID RECORD DESCRIPTION, TRY AGAIN'
[17]  ⎕WA←⎕EX 'INPT'
[18]  →(2≠1 ⎕SVO 'INPT')/ER1
[19]  INPT←'IN ',(⍕M),' ID=(DATA) MSG=OFF'
[20]  →(1≠∧/0=INPT)/ER2
[21]  I←0
[22]  READ:→(0=ρ,Δ←INPT)/ER3
[23]  →(N>I←I+1)/READ
[24]  J←1+1↑⍴,Δ[(1↓⍳1↑ρΔ);7]
[25]  →(1≠Δ[1;6])/CONTINUE
[26]  ⎕←(2ρ⎕AV[157]),(18ρ' '),'SUMMARY OF MAXIMUM PRESSURE GRADIENT',⎕AV[157]
[27]  X←,Δ[1;]÷K1
[28]  ⎕←(13ρ' '),MODEL,((Y≠' ')/Y←⎕AV[(3ρ1000)⊤X[7]]),'-',(⍕X[5]),⎕AV[157]
[29]  Y←'   C = ',(⍕X[3]),'    -PCL = ',⍕X[4]
[30]  Y←'A = ',(⍕X[1]),'     B = ',(⍕X[2]),Y
[31]  ⎕←((0⌈36-⌊(ρY)÷2)ρ' '),Y
[32]  IDN←X[5]
[33]  ' '
[34]  X←,Δ[2;]÷K4
[35]  Y←'DA = ',(⍕X[1]),'    DB = ',(⍕X[2]),'    DC = ',(⍕X[3])
[36]  ⎕←((0⌈36-⌊(ρY)÷2)ρ' '),Y,⎕AV[157]
[37]  '  SL#      X       Y       Z    BETA    S      P/PCL  DP/DS ZO-ZE BETAE BETAO
[38]  ' '
[39]  CONTINUE:→(IDN≠Δ[1;5])/(⎕LC[1]+2)
[40]  Y←Δ[1;6],((,Δ[J;]),((Δ[3;3],0)-(,Δ[(1↑ρΔ);3,4])×1,¯1),Δ[3;4])÷K4
[41]  ⎕←(5,0,9,2,6,2,6,2,6,2,6,2,7,4,7,4,6,2,6,2,6,2)⍕K2[1,(⍳7),1,4,4]×Y
[42]  →(K>I)/READ
[43]  STOP:INPT←⍳0
[44]  →(1≠∧/0=INPT)/ER4
[45]  →(2=⎕SVR 'INPT')/0
[46]  ER5:→OUT,ρ⎕←'SUMMARY: ERROR RETRACTING SHARED VARIABLE'
[47]  ER1:→OUT,ρ⎕←'SUMMARY: ERROR ESTABLISHING SHARED VARIABLE'
[48]  ER2:→OUT,ρ⎕←'SUMMARY: ERROR OPENING FILE ',⍕M
[49]  ER3:→OUT,ρ⎕←'SUMMARY: END OF FILE ',⍕M
[50]  ER4:→OUT,ρ⎕←'SUMMARY: ERROR CLOSING FILE ',⍕M
[51]  OUT:→0×ρ(⎕EX 'INPT'),(⎕SVR 'INPT')
      ∇
```

SAMPLE INPUT

X			
0	‾0.1219	‾1.6256	1
1.27	‾0.1219	‾1.6256	2
2.54	‾0.1219	‾1.6256	3
3.556	‾0.1219	‾1.6256	4
3.9421	‾0.1219	‾1.6256	5
4.3023	‾0.0744	‾1.6256	6
4.638	0.0645	‾1.6256	7
4.9263	0.2858	‾1.6256	8
5.1476	0.574	‾1.6256	9
5.2865	0.9098	‾1.6256	10
5.334	1.27	‾1.6256	11
5.334	2.54	‾1.6256	12
5.334	3.81	‾1.6256	13
5.334	5.08	‾1.6256	14
5.334	6.35	‾1.6256	15
5.334	8.89	‾1.6256	16
5.334	11.43	‾1.6256	17
5.334	13.97	‾1.6256	18
5.334	16.51	‾1.6256	19
5.334	19.05	‾1.6256	20

$((12 \rho 9\ 4),3,0) \ast \underline{A}$

| 13.5932 | 10.7950 | 1.2499 | 4.4450 | .9525 | .7620 | 3 |

RUN 1 TO 20

DO YOU WISH TO EXPUNGE SOME FUNCTIONS TO CONSERVE WS (0=N, 1=Y)
☐:
    1
DO YOU WISH TO RECORD RESULTS ON TAPE (0=N, 1=Y)
☐:
    1
ENSURE OUTPUT DATA TAPE IS ON, AND MARKED
HIT EXECUTE KEY TO CONTINUE

ENTER OUTPUT FILE NUMBER
☐:
    1
DO YOU WISH TO RECORD FROM THE BEGINNING OF THE FILE (0=N, 1=Y)
☐:
    0

-64-

SAMPLE OUTPUT

AJDE MODEL 0232 DIFFUSER CONFIGURATION B-87213 STREAMLINE NO. 1

A = 13.593   B = 10.795   C = 1.2499   -PCL = 0.00060464

DA = 4.445   DB = 0.9525   DC = 0.762

X	Y	Z	BETA	S	P/PCL	DP/DS/PCL
.0000	-.1219	-1.6256	10.224	.0000	1.1868	.0953
.0000	-.1677	-1.8796	10.721	.2581	1.1618	.0988
.0000	-.2158	-2.1336	11.216	.5166	1.1358	.1019
.0000	-.2662	-2.3876	11.708	.7756	1.1090	.1046
.0000	-.3188	-2.6416	12.198	1.0350	1.0815	.1069
.0000	-.3737	-2.8956	12.686	1.2948	1.0535	.1086
.0000	-.4309	-3.1496	13.172	1.5552	1.0250	.1100
.0000	-.4903	-3.4036	13.655	1.8160	.9962	.1108
.0000	-.5520	-3.6576	14.137	2.0774	.9671	.1113
.0000	-.6010	-3.8520	14.503	2.2779	.9448	.1114*
.0000	-.6160	-3.9116	14.615	2.3394	.9379	.1114
.0000	-.6823	-4.1656	15.092	2.6019	.9087	.1111
.0000	-.7508	-4.4196	15.566	2.8649	.8795	.1105
.0000	-.8215	-4.6736	16.039	3.1286	.8505	.1096
.0000	-.8945	-4.9276	16.509	3.3929	.8217	.1084
.0000	-.9698	-5.1816	16.976	3.6578	.7932	.1069
.0000	-1.0473	-5.4356	17.442	3.9234	.7650	.1052
.0000	-1.1271	-5.6896	17.905	4.1896	.7372	.1033
.0000	-1.2092	-5.9436	18.366	4.4565	.7099	.1012
.0000	-1.2935	-6.1976	18.825	4.7242	.6832	.0989
.0000	-1.3801	-6.4516	19.282	4.9925	.6569	.0965
.0000	-1.4690	-6.7056	19.737	5.2616	.6313	.0940
.0000	-1.5601	-6.9596	20.190	5.5315	.6063	.0914
.0000	-1.6535	-7.2136	20.640	5.8021	.5819	.0888
.0000	-1.7492	-7.4676	21.089	6.0735	.5582	.0860
.0000	-1.8472	-7.7216	21.536	6.3458	.5351	.0833
.0000	-1.9474	-7.9756	21.981	6.6188	.5127	.0805
.0000	-2.0499	-8.2296	22.424	6.8927	.4911	.0777
.0000	-2.1547	-8.4836	22.866	7.1675	.4701	.0750
.0000	-2.2619	-8.7376	23.305	7.4432	.4498	.0722
.0000	-2.3713	-8.9916	23.743	7.7197	.4302	.0695
.0000	-2.4830	-9.2456	24.179	7.9972	.4113	.0668
.0000	-2.5970	-9.4996	24.614	8.2757	.3931	.0641
.0000	-2.7134	-9.7536	25.047	8.5550	.3756	.0615
.0000	-2.8321	-10.0076	25.478	8.8354	.3587	.0589
.0000	-2.9531	-10.2616	25.908	9.1168	.3425	.0564
.0000	-3.0765	-10.5156	26.336	9.3992	.3269	.0540
.0000	-3.2022	-10.7696	26.763	9.6826	.3119	.0516
.0000	-3.3303	-11.0236	27.188	9.9670	.2976	.0493
.0000	-3.4608	-11.2776	27.612	10.2526	.2838	.0471
.0000	-3.5937	-11.5316	28.035	10.5392	.2706	.0450
.0000	-3.7289	-11.7856	28.456	10.8270	.2580	.0429
.0000	-3.8666	-12.0396	28.876	11.1159	.2459	.0409
.0000	-4.0066	-12.2936	29.295	11.4060	.2343	.0390
.0000	-4.1492	-12.5476	29.713	11.6972	.2232	.0371
.0000	-4.2941	-12.8016	30.130	11.9897	.2126	.0353
.0000	-4.4415	-13.0556	30.546	12.2834	.2025	.0336
.0000	-4.5914	-13.3096	30.960	12.5783	.1929	.0320

AJDE MODEL 0232 DIFFUSER CONFIGURATION B-87213 STREAMLINE NO. 1

$A = 13.593$ $B = 10.795$ $C = 1.2499$ $-PCL = 0.00060464$

$DA = 4.445$ $DB = 0.9525$ $DC = 0.762$

X	Y	Z	BETA	S	P/PCL	DP/DS/PCL
.0000	¯4.7438	¯13.5636	31.374	12.8745	.1836	.0304
.0000	¯4.8987	¯13.8176	31.787	13.1720	.1748	.0289
.0000	¯5.0561	¯14.0716	32.199	13.4708	.1664	.0274
.0000	¯5.2160	¯14.3256	32.610	13.7710	.1584	.0260

SUMMARY FILE FROM 21 TO 40

SUMMARY OF MAXIMUM PRESSURE GRADIENT

AJDE MODEL 0232 DIFFUSER CONFIGURATION B-87213

A = 13.593   B = 10.795   C = 1.2499   -PCL = 0.00060464

DA = 4.445   DB = 0.9525   DC = 0.762

SL#	X	Y	Z	BETA	S	P/PCL	DP/DS	ZO-ZE	BETAE	BETAO
1	.00	⁻.60	⁻3.85	14.50	2.28	.9448	.1114	12.70	32.61	10.22
2	1.32	⁻.59	⁻3.82	14.41	2.24	.9526	.1128	12.70	32.61	10.19
3	2.64	⁻.55	⁻3.72	14.15	2.14	.9766	.1173	12.70	32.68	10.11
4	3.70	⁻.51	⁻3.59	13.89	2.01	1.0090	.1234	12.70	32.96	10.05
5	4.09	⁻.49	⁻3.53	13.79	1.95	1.0251	.1264	12.70	33.16	10.03
6	4.47	⁻.42	⁻3.49	13.65	1.90	1.0389	.1292	12.70	33.22	9.96
7	4.82	⁻.26	⁻3.46	13.42	1.87	1.0485	.1312	12.70	33.02	9.79
8	5.12	⁻.01	⁻3.44	13.18	1.85	1.0536	.1324	12.70	32.73	9.57
9	5.36	.30	⁻3.45	12.97	1.86	1.0540	.1327	12.70	32.46	9.33
10	5.52	.65	⁻3.47	12.83	1.88	1.0493	.1320	12.70	32.23	9.11
11	5.59	1.02	⁻3.52	12.72	1.92	1.0393	.1303	12.70	31.96	8.89
12	5.64	2.33	⁻3.68	12.73	2.08	1.0027	.1239	12.70	31.78	8.39
13	5.70	3.64	⁻3.79	13.23	2.20	.9799	.1199	12.70	33.04	8.28
14	5.74	4.94	⁻3.87	13.99	2.29	.9653	.1174	12.70	35.15	8.38
15	5.79	6.24	⁻3.94	14.79	2.36	.9566	.1158	12.70	37.63	8.58
16	5.85	8.81	⁻4.02	16.19	2.46	.9479	.1139	12.70	42.60	9.00
17	5.89	11.38	⁻4.08	17.15	2.52	.9437	.1128	12.70	46.61	9.30
18	5.92	13.94	⁻4.12	17.71	2.56	.9414	.1121	12.70	49.33	9.49
19	5.93	16.49	⁻4.14	18.00	2.59	.9402	.1116	12.70	50.85	9.58
20	5.94	19.05	⁻4.14	18.08	2.59	.9398	.1115	12.70	51.34	9.61

PART III SERVICE PROGRAMS

```
     ∇ NZ SHAPE MNK;I;INPT;M;N;NS;K;J;JE;X;Y;Z;ZO;□PW
[1]    ⋒ FULL SYNTAX:     'NZ SHAPE FILE# FROM N1 TO N2'
[2]    ⋒ PARTIAL SYNTAX: 'NZ SHAPE FILE# FROM N1 (TO END)'
[3]    ⋒                 'NZ SHAPE FILE# (FROM 1 TO END)'
[4]    ⋒   FILE# = FILE NUMBER, N1, N2 ARE RECORD NUMBERS
[5]    ⋒   NZ = NUMBER OF Z POINTS (1.27 CM INTERVAL) RELATIVE TO ZO
[6]    ⋒ SPECIAL CASE: TYPE 'NZ SHAPE FILE' TO DISPLAY ALL SHAPES IN FILE
[7]    ⋒ GLOBAL VARS: IDN = ID# SET WHEN SL#1 IS DETECTED ( SET TABLE TO 0)
[8]    ⋒               SLN = SL# WHICH SIGNALS COMPLETION OF DATA ACQUISITION
[9]    ⋒               MODEL = MODEL DESCRIPTION; CONF = CONFIGURATION
[10]   □PW←2+6×1+NS←20
[11]   ZO←¯1.6256
[12]   Z←1.27×(⍳NZ)-1
[13]   M←(,MNK)[1]
[14]   →(M>0)/□LC[1]+2
[15]   →0
[16]   N←1
[17]   K←500
[18]   →(1=ρ,MNK)/□LC[1]+4
[19]   N←(,MNK)[2]
[20]   →(2=ρ,MNK)/□LC[1]+2
[21]   K←(,MNK)[3]
[22]   →((N≥1)∧(K≥N))/□LC[1]+2
[23]   →0,0ρ□←'INVALID RECORD DESCRIPTION, TRY AGAIN'
[24]   □WA←□EX 'INPT'
[25]   →(2≠1 □SVO 'INPT')/ER1
[26]   INPT←'IN ',(⍕M),' ID=(DATA) MSG=OFF'
[27]   →(1≠∧/0=INPT)/ER2
[28]   I←0
[29] READ:→(0=ρ,Δ←INPT)/ER3
[30]   →(N>I←I+1)/READ
[31]   JE←1↑ρΔ
[32]   J←(JE>J)/J←2+(2↓¯1↓,Δ[;3]÷100000000)⍳(ZO-Z)
[33]   →(1≠Δ[1;6])/CONTINUE
[34]   □←(2ρ□AV[157]),(46ρ' '),'SUMMARY OF DIFFUSER WALL COORDINATES',□AV[157]
[35]   X←(,Δ[1;])÷(3ρ100000000),10000000000,1,1,1
[36]   □←(42ρ' '),MODEL,((Y≠' ')/Y←□AV[(3ρ1000)⊤X[7]]),'-',(⍕X[5]),□AV[157]
[37]   Y←(,Δ[2;])÷100000000
[38]   Y←'   DA = ',(⍕Y[1]),'   DB = ',(⍕Y[2]),'   DC = ',(⍕Y[3])
[39]   Y←'   C = ',(⍕X[3]),Y,'   -PCL = ',⍕X[4]
[40]   Y←'A = ',(⍕X[1]),'   B = ',(⍕X[2]),Y
[41]   □←((0⌈64-⌊(ρY)÷2)ρ' '),Y
[42]   IDN←X[5]
[43]   □←□AV[157],('     Z  ',(6 0)⍕⍳NS)
[44]   Δ←(3,(NZ+1),NS)ρ⌊0
[45] CONTINUE:→(IDN≠Δ[1;5])/COUNT
[46]   Δ[1;;Δ[1;6]]←(1,(NZ+1),1)ρ(NZ↑,Δ[J;1]),Δ[JE;1]
[47]   Δ[2;;Δ[1;6]]←(1,(NZ+1),1)ρ(NZ↑,Δ[J;2]),Δ[JE;2]
[48]   Δ[3;;Δ[1;6]]←(1,(NZ+1),1)ρ(NZ↑,Δ[J;3]),Δ[JE;3]
[49]   →(SLN≠Δ[1;6])/COUNT
[50]   J←1
```

```
[51] PRINT:[]←' '
[52]    →(J≠NZ+1)/[]LC[1]+2
[53]    →[]LC[1]+2+0×ρρ[]←'           X',(6 2)⊤Δ[1;J;]÷100000000
[54]    []←((6 2)⊤Z[J]),' X',(6 2)⊤Δ[1;J;]÷100000000
[55]    []←'           Y',(6 2)⊤Δ[2;J;]÷100000000
[56]    →(J≠NZ+1)/[]LC[1]+3
[57]    []←'           Z',(6 2)⊤-(Δ[3;J;]÷100000000)-Z0
[58]    []←2ρ[]AV[157]
[59]    →((NZ+1)≥J←J+1)/PRINT
[60] COUNT:→(K>I)/READ
[61] STOP:INPT←ι0
[62]    →(1≠∧/0=INPT)/ER4
[63]    →(2=[]SVR 'INPT')/0
[64] ER5:→OUT,ρ[]←'SHAPE: ERROR RETRACTING SHARED VARIABLE'
[65] ER1:→OUT,ρ[]←'SHAPE: ERROR ESTABLISHING SHARED VARIABLE'
[66] ER2:→OUT,ρ[]←'SHAPE: ERROR OPENING FILE ',⊤M
[67] ER3:→OUT,ρ[]←'SHAPE: END OF FILE ',⊤M
[68] ER4:→OUT,ρ[]←'SHAPE: ERROR CLOSING FILE ',⊤M
[69] OUT:→0×ρ([]EX 'INPT'),([]SVR 'INPT')
     ∇


     ∇ R←M FROM N
[1]    R←M,N
     ∇


     ∇ R←N TO K
[1]    R←N,K
     ∇
```

10 SHAPE 1 FROM 21 TO 40

SUMMARY OF DIFFUSER WALL COORDINATES

AJDE MODEL 0232 DIFFUSER CONFIGURATION B-87213

A = 13.573   B = 10.795   C = 1.2499   DA = 4.445   DR = 0.9525   DC = 0.762   -PCL = 0.00060464

Z		1	2	3	4	5	6	7	8	9	10	11	12	13	14	15	16	17	18	19	20
.00	X	.00	1.27	2.54	3.56	3.94	4.30	4.64	4.93	5.15	5.29	5.33	5.33	5.33	5.33	5.33	5.33	5.33	5.33	5.33	5.33
	Y	-.12	-.12	-.12	-.12	-.12	-.07	.06	.29	.57	.91	1.27	2.54	3.81	5.08	6.35	8.89	11.43	13.97	16.51	19.05
1.27	X	.00	1.30	2.60	3.64	4.04	4.41	4.75	5.05	5.29	5.44	5.49	5.51	5.52	5.54	5.55	5.57	5.58	5.58	5.59	5.59
	Y	-.37	-.37	-.35	-.36	-.35	-.30	-.15	.09	.39	.74	1.11	2.42	3.72	5.01	6.29	8.85	11.40	13.95	16.50	19.05
2.54	X	.00	1.33	2.67	3.75	4.16	4.55	4.91	5.23	5.47	5.64	5.70	5.74	5.78	5.81	5.84	5.89	5.92	5.93	5.94	5.94
	Y	-.68	-.68	-.66	-.64	-.63	-.57	-.41	-.15	.17	.54	.92	2.28	3.61	4.92	6.23	8.81	11.38	13.94	16.49	19.05
3.81	X	.00	1.38	2.77	3.88	4.31	4.72	5.10	5.44	5.71	5.89	5.96	6.03	6.10	6.16	6.22	6.30	6.35	6.38	6.40	6.40
	Y	-1.05	-1.04	-1.01	-.98	-.96	-.89	-.71	-.44	-.09	.30	.71	2.11	3.48	4.83	6.15	8.76	11.35	13.92	16.49	19.05
5.08	X	.00	1.43	2.88	4.05	4.50	4.92	5.33	5.69	5.98	6.18	6.27	6.38	6.48	6.53	6.67	6.30	6.89	6.94	6.96	6.97
	Y	-1.47	-1.46	-1.42	-1.37	-1.34	-1.26	-1.06	-.76	-.39	.02	.45	1.92	3.34	4.72	6.07	8.71	11.31	13.90	16.48	19.05
6.35	X	.00	1.50	3.01	4.23	4.71	5.16	5.59	5.98	6.30	6.52	6.63	6.78	6.93	7.07	7.20	7.40	7.53	7.60	7.64	7.65
	Y	-1.95	-1.93	-1.88	-1.81	-1.77	-1.67	-1.46	-1.13	-.73	-.29	.17	1.71	3.18	4.60	5.97	8.65	11.28	13.68	16.46	19.05
7.62	X	.00	1.57	3.15	4.45	4.95	5.43	5.89	6.31	6.66	6.91	7.03	7.23	7.43	7.62	7.80	8.08	8.27	8.39	8.43	8.45
	Y	-2.48	-2.46	-2.39	-2.30	-2.26	-2.14	-1.90	-1.55	-1.11	-.64	-.15	1.46	2.99	4.46	5.87	8.59	11.24	13.85	16.45	19.05
8.89	X	.00	1.64	3.31	4.68	5.21	5.72	6.22	6.68	7.06	7.33	7.48	7.74	7.99	8.24	8.48	8.86	9.12	9.28	9.36	9.39
	Y	-3.08	-3.05	-2.96	-2.85	-2.80	-2.67	-2.40	-2.01	-1.54	-1.03	-.51	1.19	2.79	4.30	5.75	8.51	11.19	13.82	16.44	19.05
10.16	X	.00	1.73	3.49	4.94	5.51	6.05	6.59	7.09	7.50	7.80	7.97	8.29	8.61	8.93	9.23	9.74	10.10	10.32	10.43	10.47
	Y	-3.73	-3.69	-3.59	-3.45	-3.39	-3.24	-2.94	-2.52	-2.01	-1.46	-.91	.89	2.55	4.12	5.61	8.43	11.13	13.79	16.42	19.05
11.43	X	.00	1.83	3.69	5.22	5.83	6.41	6.98	7.52	7.97	8.31	8.51	8.89	9.29	9.68	10.06	10.72	11.20	11.51	11.67	11.72
	Y	-4.44	-4.40	-4.28	-4.12	-4.04	-3.87	-3.55	-3.08	-2.53	-1.94	-1.35	.55	2.29	3.91	5.45	8.33	11.07	13.75	16.40	19.05
	X	.00	1.93	3.90	5.53	6.17	6.79	7.41	7.99	8.49	8.87	9.08	9.54	10.02	10.50	10.97	11.81	12.45	12.87	13.10	13.17
	Y	-5.22	-5.17	-5.02	-4.84	-4.75	-4.56	-4.20	-3.70	-3.10	-2.46	-1.84	.18	2.00	3.68	5.27	8.21	11.00	13.70	16.38	19.05
	Z	12.70	12.70	12.70	12.70	12.70	12.70	12.70	12.70	12.70	12.70	12.70	12.70	12.70	12.70	12.70	12.70	12.70	12.70	12.70	12.70

```
      ∇ PLOT SCALE;Δ;XO;X1;J;JE;K;N;NS;I;XCL;YMP;ZCL;ZO;NULL;P
[1]   A REQUIRED PROCEDURE:
[2]   A 1. USE )PATCH FROM IBM 5100 APL GRAPHPAK
[3]   A 2. RUN ∇SHAPE FIRST, WITH AID OF DATA TAPE, TO GET Δ
[4]   A EXAMPLE: PLOT 0.5 (FOR HALF CM SCALE)
[5]    ZO←¯162.56+0×YMP←1905
[6]    XCL←⌊1399.5-1140×SCALE←SCALE÷2.54
[7]    ZCL←⌊0.5+XCL-1105×SCALE
[8]    NULL←⌊0.5+(YMP×SCALE),0
[9]    Δ←(ρΔ)ρ⌊0
[10]   Δ[1;;]←⌊1⌊0.5+SCALE×(Δ[2;;]÷1000000)-YMP
[11]   Δ[2;;]←⌊0.5+0.69818×S̄CALE×(Δ[1;;]÷1000000)
[12]   Δ[3;;]←⌊0.5+ZCL+0.69818×SCALE×(Δ[3;;]÷1000000)-ZO
[13]   NS←(,ρΔ)[3]
[14]   JE←(,ρΔ)[2]
[15]   ⎕WA←1 ⎕SVO 'P'
[16]   P←'OUT 51001'
[17]   P←⊤2,Δ[1;1;NS],(XCL+Δ[2;1;NS]),Δ[1;1;NS],(XCL-Δ[2;1;NS]),4,3,0
[18]   P←⊤2,Δ[1;1;NS],XCL,Δ[1;1;1],XCL,4,3,0
[19]   I←1
[20] IMAGE:N←¯1*(I+1)
[21]   J←1
[22] CONTOUR:XO←,Δ[1,2;J;1]
[23]   K←2
[24] TOPVIEW:X1←,Δ[1,2;J;K]
[25]   →((∧/NULL=XO)∨(∧/NULL=X1))/⎕LC[1]+2
[26]   P←⊤2,((4ρ0,XCL)+(4ρ1,N)×XO,X1),1,1,0
[27]   →(NS≥K←K+1+0×ρρXO←X1)/TOPVIEW
[28]   →(JE≥J←J+1)/CONTOUR
[29]   K←1
[30] STREAMLINE:XO←,Δ[1,2;1;K]
[31]   J←2
[32] RIB:X1←,Δ[1,2;J;K]
[33]   →(∧/NULL=X1)/⎕LC[1]+3
[34]   P←⊤2,((4ρ0,XCL)+(4ρ1,N)×XO,X1),1,1,0
[35]   XO←X1
[36]   →(JE≥J←J+1)/RIB
[37]   →(NS≥K←K+1)/STREAMLINE
[38]   →(2≥I←I+1)/IMAGE
[39]   P←⊤2,Δ[1;1;NS],Δ[3;JE;NS],Δ[1;1;NS],ZCL,4,3,0
[40]   P←⊤2,Δ[1;1;NS],ZCL,Δ[1;1;1],ZCL,4,3,0
[41]   XO←,Δ[1,3;1;1]
[42]   J←2
[43] CUTVIEW:X1←,Δ[1,3;J;1]
[44]   →(∧/NULL=,Δ[1,2;J;1])/⎕LC[1]+3
[45]   P←⊤2,XO,X1,1,1,0
[46]   XO←X1
[47]   →(JE≥J←J+1)/CUTVIEW
[48]   XO←,Δ[1,3;JE;1]
[49]   K←2
[50] SIDEVIEW:X1←,Δ[1,3;JE;K]
[51]   P←⊤2,XO,X1,1,1,0
[52]   →(NS≥K←K+1+0×ρρXO←X1)/SIDEVIEW
[53]   P←⍳0
[54]   ⎕WA←⎕SVR 'P'
      ∇
```

DISTRIBUTION FOR FINAL REPORT NADC 77050-30

Copies Enc.	Address	Copies Encl.	Address

7   Commander
Naval Air Development Center
Warminster, PA 18974
    (2)   Attn: Mr. C. Mazza (Code 6053)
    (2)   Attn: Dr. K. Green (Code 6052)

5   Commander
Naval Air Systems Command
Jefferson Plaza
Washington, D. C. 20361
    (1)   Attn: Mr. L. Koven (03E)
    (3)   Attn: Mr. R. Siewert (AIR 320D)
    (1)   Attn: Mr. R. Brown (AIR 330D)

1   Commander
Naval Weapons Center
China Lake, CA 93555
Attn: B. Kowalsky (Code 36604)

2   Commander
Naval Ship Research and Development
Center
Carderock, MD 20034
    (1)   Attn: Mr. R. Murphy
    (1)   Attn: Dr. T. C. Tai

1   Commander
Naval Air Propulsion Test Center
Trenton, NJ 98628
Attn: Mr. L. Palcza

1   Commander
U. S. Naval Academy
Annapolis, MD 21402
Attn: Mr. J. Sladky

2   Chief
Office of Naval Research
800 N. Quincy Street
Arlington, VA 22217
    (1)   Attn: Dr. R. Whitehead
    (1)   Attn: Mr. K. Ellingsworth

1   Superintendent
Naval Postgraduate School
Monterey, CA 93940
Attn: Dr. M. Platzer

12   Defense Documentation Center
Building #5
Cameron Station
Alexandria, VA 22314

1   NASA-Ames Research Center
40 x 80 Wind Tunnel
Moffett Field, CA 94035
Attn: Mr. D. Koenig (MS-247-1)

1   Director
Air Force Flight Dynamics Lab.
AFFDL/FXM
Wright-Patterson AFB
Dayton, OH 45433
Attn: Dr. K. Nagaraja

1   Vought Corporation
Advance Technology Center, Inc.
P. O. Box 6144
Dallas, TX 75221
Attn: Dr. C. Haight

1   General Dynamics Corporation
Fort Worth, TX 76101
Attn: Mr. J. Clifton (MS-2892)

1   Rockwell International
Columbus, OH 43216
Attn: Dr. P. Bevilaqua

1   Rockwell International Science
Center
1049 Camino Dos Rios
P. O. Box 1085
Thousand Oaks, CA 91360
Attn: Dr. N. Malmuth

1   Grumman Aerospace Corporation
Bethpage, Long Island, New York
11714
Attn: Dept. 420, Plant 35

1   Flight Dynamics Research Corp.
15809 Stagg Street
Van Nuys, CA 91406
Attn: Dr. M. Alperin

1   Computational Mechanics
3601A Chapman Highway
Knoxville, TN 37920
Attn: Dr. J. Baker